



# Hydrogeochemical and isotopic assessment for characterizing groundwater quality in the Mitidja plain (northern Algeria)

Samir Yahiaoui<sup>1</sup> · Mohamed Meddi<sup>1</sup> · Moumtaz Razack<sup>2</sup> · Abdelmadjid Boufekane<sup>1,3</sup> · Belkacem Samir Bekkoussa<sup>4</sup>

Received: 2 January 2023 / Accepted: 23 May 2023 / Published online: 8 June 2023  
© The Author(s), under exclusive licence to Springer-Verlag GmbH Germany, part of Springer Nature 2023

## Abstract

Coastal aquifer overexploitation represents a concerning trigger for water salinization around the world and especially in arid and semi-arid regions along with urban growth and urbanization, as well as land use human-induced changes. This study aims to assess the groundwater quality in the Mitidja alluvial aquifer (northern Algeria) along with its suitability for domestic and agricultural utilizations. A hydrogeochemical approach, based on the interpretation of groundwater physicochemical parameters (EC, pH, dry residue,  $\text{Ca}^{2+}$ ,  $\text{Mg}^{2+}$ ,  $\text{Na}^+$ ,  $\text{K}^+$ ,  $\text{Cl}^-$ ,  $\text{SO}_4^{2-}$ ,  $\text{HCO}_3^-$ , and  $\text{NO}_3^-$ ) collected during the wet and dry periods for the years 2005 and 2017 along with an isotopic characterization, including stable isotopes to identify the recharge sources for the samples collected in October 2017, has been proposed. The results show the presence of three dominant hydrochemical facies: (i) calcium chloride, (ii) sodium chloride, and (iii) calcium bicarbonate. Groundwater mineralization and salinization are so ascribable carbonates and evaporitic dissolution, especially during the dry periods, and to the presence of seawater. Ion exchange significantly affects groundwater chemistry along with human activities which directly or indirectly contribute in raising groundwater salts concentration. Specifically,  $\text{NO}_3^-$  concentrations are very high in the eastern portion of the study area which is exposed to fertilizers pollution where also the Richards classification pointed out the necessity of limit water utilization for agricultural use. The  $\delta^2\text{H} = f(\delta^{18}\text{O})$  diagram indicates that the recharge origin for this aquifer is mainly due to the oceanic meteoric rainwater from the Atlantic and the Mediterranean Sea. The methodology proposed in this study can be applied in the similar worldwide coastal areas in order to contribute and sustainable water resource management in these regions.

**Keywords** Mitidja alluvial plain · Groundwater quality · Hydrogeochemistry · Isotopic tool

## Introduction

The world's population has changed dramatically from 2.6 billion in 1950 to almost 8 billion in 2022 (United Nations 2022). This population growth, particularly in the major

urban regions, inevitably leads to increasing economic and social needs. This is characterized by the great wave of industrialization and the increased demand for agricultural production. As a result, global water use has increased six-fold over the past 100 years and continues to increase steadily by about 1% per year (United Nations 2018). The use of this precious resource is expected to continue to increase globally, driven not only by population growth but also by economic development and changing consumption patterns (United Nations 2018). However, this resource is becoming increasingly scarce and coveted. More than 80% of the world's wetlands have been lost since the pre-industrial era, and over the past 20 years, the water stock on land has decreased by one centimeter per year, taking into account surface, sub-surface, soil moisture, snow, and ice. In total, the number and duration of drought have increased by 29% in 20 years (WMO 2021).

---

Responsible Editor: Xianliang Yi

### Highlights

- Hydrogeochemistry and stable isotopes were employed to assess the groundwater quality in the Mitidja plain (northern Algeria).
- Groundwater mineralization is due to the dissolution of carbonates and evaporitic formations, especially during the dry periods.
- Seawater intrusion and nitrate contamination constitute a significant threat in the study area for the agricultural purposes.

---

Extended author information available on the last page of the article

Groundwater makes up almost 99% of the world's total liquid freshwater supply and currently accounts for a quarter of all freshwater used by humans. Large volumes of freshwater are found throughout the world beneath the surface of the land, but their abundance varies considerably from place to place (UNESCO 2022). These groundwater resources play an essential role in meeting society's basic needs, such as human consumption and industrial and agricultural needs, with the latter accounting for almost 70% of the available resources. According to UNEP (1999), almost one third of the world's population uses groundwater, particularly in developing countries. However, overexploitation is creating enormous pressure on this vital resource due to increasing demand, as well as decreasing natural recharge related to decreasing precipitation in recent decades (Chabaca et al. 2007). The Maghreb countries, like all the others in the Mediterranean basin, have experienced a decrease in rainfall since the 1970s (Meddi and Hubert 2003; Bouderbala and Hadj Mohamed 2020). Uncontrolled discharges of urban and industrial effluents are frequent sources of point-source groundwater pollution. In addition, the disproportionate use of fertilizers and pesticides in agriculture directly affects the quality of aquifers (Scanlon et al. 2007; Bouderbala and Hadj Mohamed 2020).

In Algeria, particularly in the northern region of the country where the Mitidja plain is located, water resources are limited, vulnerable, and spatially unevenly distributed. Indeed, for more than two decades, anthropogenic changes have been observed in the area, such as the large wave of urbanization which has led to the sealing of soils in this region, as well as the overexploitation of the water table caused mainly by the decrease in rainfall observed since 1975 (Meddi and Hubert 2003; Zeroual et al. 2016). We also note the construction of several surface water storage and transfer works which considerably limit the recharge of the aquifer and lead to a drop in piezometric levels. In addition, the multiplication of uncontrolled discharge points emanating from large urban clusters and industrial zones that are constantly multiplying across the area (Ait Ouali 2007). However, another problem that accentuates the pollution of groundwater is the careless use of fertilizers and pesticides in hydro-agricultural operations, which considerably affects the underlying water table (DSA-Blida 2003). These so-called anthropogenic changes are also accompanied by certain natural changes visible in the image of the climatic hazards recorded in the region and the intrusion of sea water through its northeastern part; more exactly in the Algiers bay. This delicate situation, illustrated by the drop in groundwater levels and the risks of pollution it faces, inevitably requires new actions to be taken in order to exploit this underground resource in a rational manner.

The groundwater of the Mitidja aquifer contributes to the drinking water supply of many localities in the capital as

well as several cities located in the plain. They also ensure the irrigation of tens of thousands of hectares and the supply of almost all industrial units (Hadjoudj et al. 2014; Zamiche 2019). Therefore, special attention must be paid to groundwater quality in the context of sustainable and integrated groundwater management. Knowledge of the physical and chemical properties of plain water is important to determine the origin of the chemical composition of groundwater (Adams and Greeley 2000).

Such an effort requires consultation between all actors and decision-makers in the sectors concerned and the research community, which must be able to provide more information and results that can be used as decision-making tools (Messahel and Benhafid 2007). The aim is not only to understand the functioning of groundwater systems and to better quantify them, but also to detect the sources of problems related to quality and to be able to intervene and act accordingly.

These problems affect many aquifers around the world and particularly in Mediterranean countries (Bachtouli and Comte 2019; Bouaissa et al. 2021; Bouaissa et al. 2022). Many regions of the world have experienced the problems of water pollution from domestic and industrial discharges, as well as excessive use of fertilizers in agriculture (Adimalla et al. 2018; Bouteldjaoui et al. 2020).

To this context, this study aims to characterize the physicochemical properties, to evaluate the groundwater quality in the Mitidja alluvial plain and its appropriateness for domestic and agricultural use, as well as to identify the sources of recharge using isotopic technique which was carried out from the data values of stable water isotopes ( $^{18}\text{O}$  and  $^2\text{H}$ ) taken in the dry period of the year 2017.

## Study region

### Broad view of the study area

Mitidja plain is located just to the south of Algiers City (Fig. 1). WSW–ENE trending and with an average altitude of 100 m, it occupies an area of 1500 km<sup>2</sup> which represents 3% of northern Algeria's surface with an average length of 100 km and an average width of 10 to 18 km. It is located between the longitudes 2°32'00" and 3°19'00" East and latitudes 36°25'17" and 36°47'40" North. It is limited to the south by the Blidean Atlas piedmonts. This plain encompasses the cities of Algiers, Blida, Tipaza, and Boumerdes.

Mitidja region enjoys a Mediterranean climate marked by a dry and hot summer and a wet and cold winter. Mean annual temperature is estimated at 18 °C; average annual rainfall is about 660 mm. Potential evapotranspiration is estimated at 501 mm or 79% of rainfall.

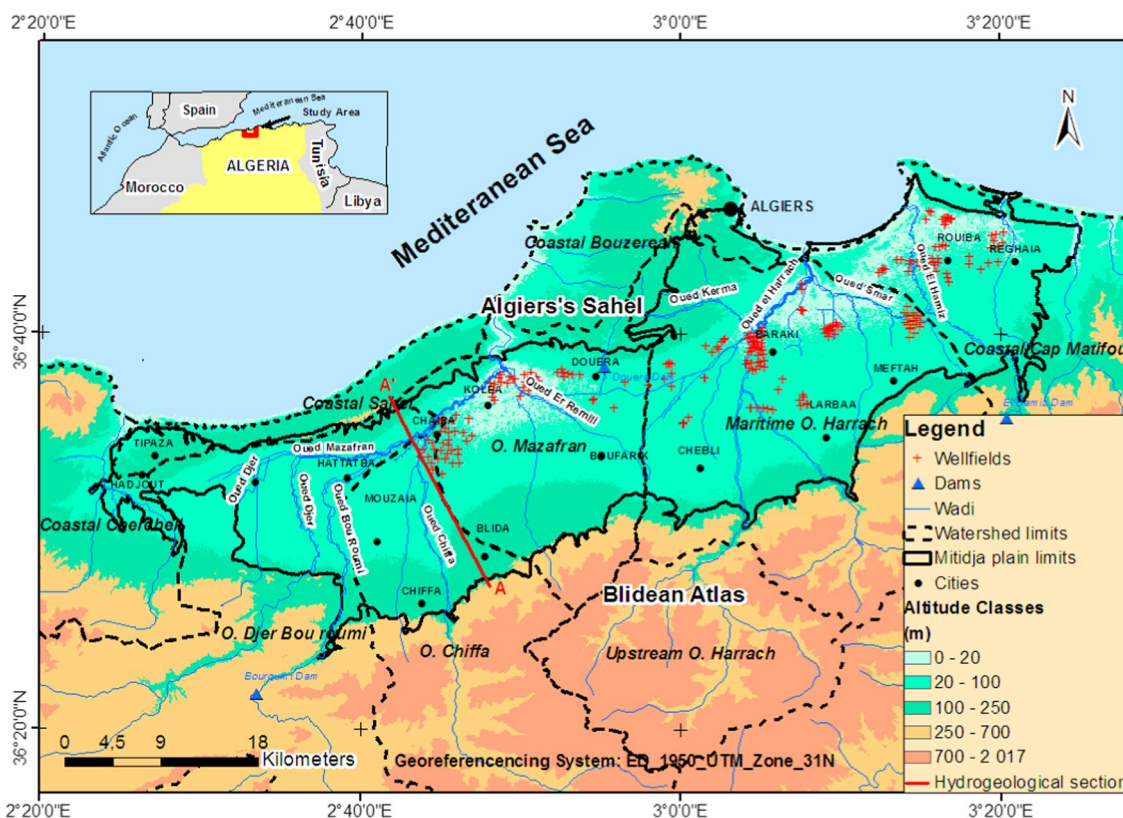


Fig. 1 Location map of Mitidja plain

The important agricultural activities in Mitidja plain are arboriculture and vegetable production, while the Sahel, situated in the north of the plain, is characterized by a forest covers (Ouradi 2014; Semmoud and Ladhem 2015). The total population in the Mitidja plain was about 3.9 million inhabitants in 2021. The population density is below 62 inhabitants per km<sup>2</sup>. The highest urban concentrations are in the center and the east of the plain. The majority of industrial activities are grouped in the center and east of the plain (Larbaa, Rouiba, Reghaia, Blida, El-Harrach and Boufarik localities).

The groundwater resource in the quaternary aquifer of the Mitidja is estimated at 259.26 Mm<sup>3</sup>; it is recharged seasonally by rainwater (Ait Ouali 2007). The main wellfields are located in the west (Mazafran I and II), in the center (Barraki), and in the east (Hamiz). However, surface water is stored, essentially, by three dams located in the plain: Hamiz, Boukerdene, and Bouroumi dams with a capacity of 15.6 Mm<sup>3</sup>, 90 Mm<sup>3</sup>, and 200 Mm<sup>3</sup>, respectively. However, the increase in population and the presence of vast fertile irrigable areas in their major parts generate a growing demand for water which has led to groundwater overexploitation (Zamiche 2019).

### Geological and hydrogeological contexts

Mitidja plain is an intermont collapse basin filled with deposits of Plio-Quaternary age. The lithostratigraphy of this plain reveals the following succession: (1) the primary basement outcrops mainly in the north part (Algiers) and in the west end part (Chenoua region) of the study area. It is consisted by a highly metamorphic gneissic basement; (2) the Mesozoic mainly outcrops in the southwest of the study area. It is composed by limestones (Jurassic age), limestones and sandstones (Neocomian and Aptian ages), and marls and limestones (Upper Albian to Senonian age); (3) the Tertiary is represented in the east and southeast by marls of Vindobonian and including the limestone lenses of Miocene which outcrop in the Blidean Atlas. Moreover, the Tertiary is made up of eruptive rocks which outcrop in the southwest boundary of Mitidja, where they are in contact with recent alluvium from Mitidja basin. On its southern and western borders, the existence of calc-alkaline volcanism dated from 11 to 16 million years is reported, showing evidence of the opening by east–west collapse of the basin during the Miocene (Bellon et al. 1977); (4) the Plaisancian corresponds to the sediments of the deep environment which settled on an erosion surface

with an average thickness of 200 m. It outcrops at surface and is only found in the Sahel hills (Fig. 2) at the core of an anticlinal folding and in the east where they constitute the eastern closure of the basin (Rivoirard 1952); (5) the Astian formation comprises several facies separated by a 4-m glauconitic key bed to a few centimeters thick, the most frequently encountered lithologies are the following: limestones or sandy limestones, sandstones, yellow limestone clays, and reef facies limestone. The average thickness of the Astian varies between 100 and 130 m; it is generally located at depths ranging from 250 to 300 m below Mitidja soil surface. In the east of the study area (Rouïba region), it is found at low depths because the erosion has been very important (Glangeaud and Aymé 1935). The outcrops of the Astian meet on the southern side of the Sahel and in the southern suburbs of Algiers, and (6) the Quaternary alluvial aquifer is mainly composed by sands, gravels alternating with silts, and clays. Apart from Mazafran's area in the west, this aquifer is entirely unconfined and lies on El-Harrach's yellow marls. Its thickness varies from 100 to 200 m. Its eastern and western limits are ensured by the uplifting of the Pleistocene' blue marl formation. This aquifer which piezometric level varies between 4 and 40 m, at depth below soil surface, is the main groundwater reservoir for the region. Its recharge originates mainly not only from rainfall, but also from the infiltrations through the beds and banks of the wadis that flow in this area.

The lithostratigraphic analysis shows two main aquifer systems: the Quaternary alluvium (Soltano-Tensiftian age or Mitidja formation) and the sandstone-limestone formations of the Astian, which rests on the Plaisancian marls forming the watertight boundary of almost the entire basin. These two aquifers are separated by the semi-permeable Villafranchian formation (yellow marls), called the El Harrach marls.

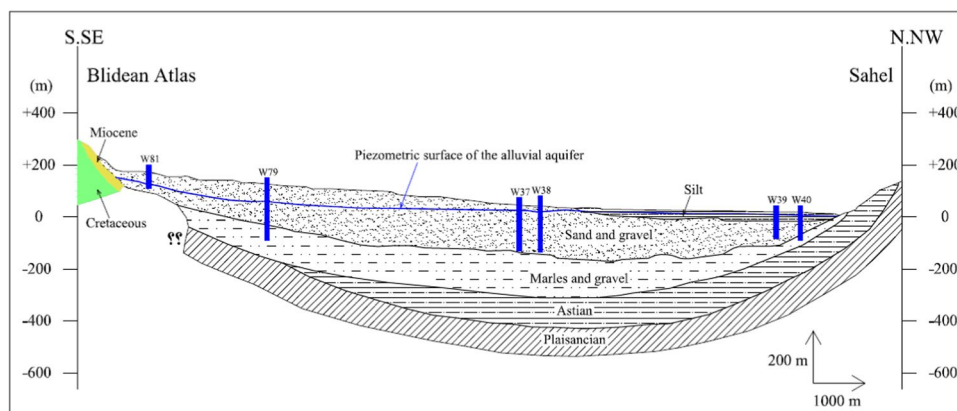
The Astian reservoir extends all most of the plain at depths ranging from 200 to 400 m. It is mainly supplied by the effective infiltration of rain in the Blidean Atlas

piedmonts. The Astian is also recharged by leakage from the Mitidja groundwater through the semi-permeable Villafranchian formation (the yellow marls). This formation is not very thick and displays a permeability varying from  $10^{-7}$  to  $10^{-8}$  m/s. Furthermore, the average thickness of Mitidja Plio-Quaternary aquifer is around about 100 to 200 m and gets thinner towards the plain bordering; it reaches 40 m to the north at Algiers bay. This aquifer has hydrodynamic characteristics of special interest, and that is the most needed in the region. It is recharged by infiltration of precipitation falling on the plain, infiltration from wadis crossing the plain, except Reghaïa wadi (in the east), and probably vertical ascending leakage from the Astian aquifer.

The transmissivity values in the Astian aquifer range between  $0.8 \times 10^{-4}$  and  $2.9 \times 10^{-3}$  m<sup>2</sup>/s, i.e., permeability between  $4 \times 10^{-6}$  and  $1.6 \times 10^{-4}$  m/s. It includes nevertheless channels of good transmissivities with values ranging from 10 to  $30 \times 10^{-3}$  m<sup>2</sup>/s, lining up most often with transmissive channels of the alluvial aquifer (SOGREAH 2009). Storage coefficient values vary from  $5 \times 10^{-3}$  to  $5 \times 10^{-6}$  in confined areas and from 0.03 to 0.05 in unconfined areas (SOGREAH 2009). This aquifer is generally considered as confined, except in areas where it outcrops.

According to the values acquired since 1968, Mitidja alluvial aquifer transmissivity ranges between  $1 \times 10^{-4}$  and  $2 \times 10^{-2}$  m<sup>2</sup>/s (SOGREAH 2009). Often, they reach very high values, especially in the eastern part, where large wadis deposits coarse materials are found. There are three areas zones of hydrogeological interest in the study area: (i) The first zone is situated in the east (El Hamiz region) where transmissivity varies between  $1.7 \times 10^{-2}$  and  $2.3 \times 10^{-2}$  m<sup>2</sup>/s, (ii) the second zone is located in the center (El Harrach region) where transmissivity varies between  $0.4 \times 10^{-2}$  and  $3 \times 10^{-2}$  m<sup>2</sup>/s, and (iii) the third zone is located in the west (Mazafran region) where transmissivity ranges from  $1.5 \times 10^{-2}$  to  $2 \times 10^{-2}$ . However, the low values are found in low permeability zones along the axis of the west to the center and the Blidean Atlas piedmonts. These zones of low

**Fig. 2** Hydrogeological section AA' in the Mitidja plain (refer to Fig. 1 for location) (Boufekane et al. 2021)



transmissivities correspond to the places where the marls top is topographically raised.

The storage coefficient values vary from  $10^{-3}$  in confined parts of the aquifer to 0.15 in unconfined parts (SOGREAH 2009) where the vertical permeability for the Mitidja alluvial aquifer is about  $6 \times 10^{-6}$  m/s and for the Astian aquifer about  $10^{-5}$  m/s.

## Materials and methods

### Sampling and analysis techniques

The hydrogeochemical study of the Mitidja groundwater was performed using physicochemical data (cations, anions, dry residues, and electrical conductivity) measured on samples collected wet and dry periods of years 2005 (54 samples) and 2017 (50 samples).

Data were collected from a large sampling network selected so that the wells are representative with regard to the spatial and temporal variability of groundwater quality. Water samples were taken by the National Agency for Hydraulic Resources (ANRH) from wells, located in the Mitidja Plio-Quaternary aquifer. Four sampling campaigns were carried out during the two years 2005 and 2017 according to the wet (WP) and dry (DP) periods of each year. The collected sample number for each period is as follows: 20 samples during the WP/2005, 34 samples during DP/2005, 22 samples during WP/2017, and 28 samples during DP/2017.

The piezometric evolution study was performed based on the head data collected in April and September 2005 and May and October 2017, where the months of April and May correspond to the wet period (WP) and the months of September and October correspond to the dry period (DP).

The groundwater samples were collected after 15 min minimum of pumping, respecting the sampling instructions and minimize any risk of pollution. The temperature, pH, and electrical conductivity (EC) were measured in situ using WTW ProfiLine 340i Universal multi-parameter portable instrument. The samples were taken according to standardized techniques, using polyethylene bottles with a capacity of 1 L (Barcelona et al. 1985). The groundwater samples were transported in coolers at 4 °C, and the analyses were performed according to the methods approved by Rodier et al. (2009) at the laboratory of the National Hydraulics Resource Agency. The cations ( $\text{Ca}^{2+}$ ,  $\text{Mg}^{2+}$ ,  $\text{Na}^+$  and  $\text{K}^+$ ) were acidified with 1%  $\text{HNO}_3^-$  and analyzed using a flame emission spectrometry (CORNING Model 410 Flame Photometer). The anions ( $\text{Cl}^-$ ,  $\text{SO}_4^{2-}$ ,  $\text{HCO}_3^-$  and  $\text{NO}_3^-$ ) and dry residue were determined by ion chromatography method (Dionex ICS 1100). The accuracy of all chemical analysis was verified by calculating the ionic equilibrium

errors, which are generally within  $\pm 5\%$  (American Public Health Association 2005). However, isotopic measurements ( $^{18}\text{O}$  and  $^2\text{H}$ ) were realized at the Algiers Nuclear Research Center (CRNA) using a Laser Picarro-L2110i spectrometer. Analyses were processed under LIMS (Laboratory Information Management System). The analytical uncertainties on the measurements were 0.36‰ for deuterium ( $^2\text{H}$ ) and 0.05‰ for oxygen-18 ( $^{18}\text{O}$ ).

Finally, the results obtained in this study were analyzed, interpreted, and presented in the form of tables and thematic maps to give an idea about the groundwater quality and their spatial evolution using statistical analysis (XLstat software, version 2016.2), hydrogeochemistry presentation (Diagrammes software, version 6.77), calculation of water mineral saturation indices (PHREEQC software, version 2.0), and cartography of the results (ArcGis software, version 10.8).

### Methodological steps of the research process

Figure 3 shows the general flowchart that summarizes the methodology utilized in this study. The work begins with the study area presentation in its different contexts: geographical, geological, and hydrogeological. A work of sampling and analysis of the physicochemical, piezometric, and isotopic parameters was carried out until the identification and validation of the reliability of the samples collected. Statistical and geostatistical analyses, hydrochemical facies, and piezometric studies were contributed to characterize the mineralization process of groundwater. Also, isotopic tool based on the analysis of stable isotopes ( $^{18}\text{O}$  and  $^2\text{H}$ ) was carried out in order to determine the recharge sources of groundwater. Finally, the quality assessment of Mitidja groundwater defined their suitable for domestic and agricultural use.

### Groundwater hydrochemistry and controlling processes

The hydrochemistry of the Mitidja Plio-Quaternary aquifer was assessed using statistical and graphical methods. Descriptive and correlative statistics were used to evaluate the quality of the data set and search for relationships between the physicochemical parameters. Hydrochemical facies and their evolution were investigated using graphical tools as Piper diagram (Piper 1944).

To assess the processes controlling groundwater mineralization and the sources of salinity, various methods were utilized. Binary diagrams, such as  $\text{Na}^+$  vs  $\text{Cl}^-$ ,  $\text{Ca}^{2+} + \text{Mg}^{2+}$  vs  $\text{HCO}_3^- + \text{SO}_4^{2-}$ , and  $(\text{Na}^+/\text{Cl}^-)$  vs dry residue were plotted to identify rock-water interactions and the evaporation role.

Mineral saturation indices are very useful for groundwater quality assessment considering that water chemistry

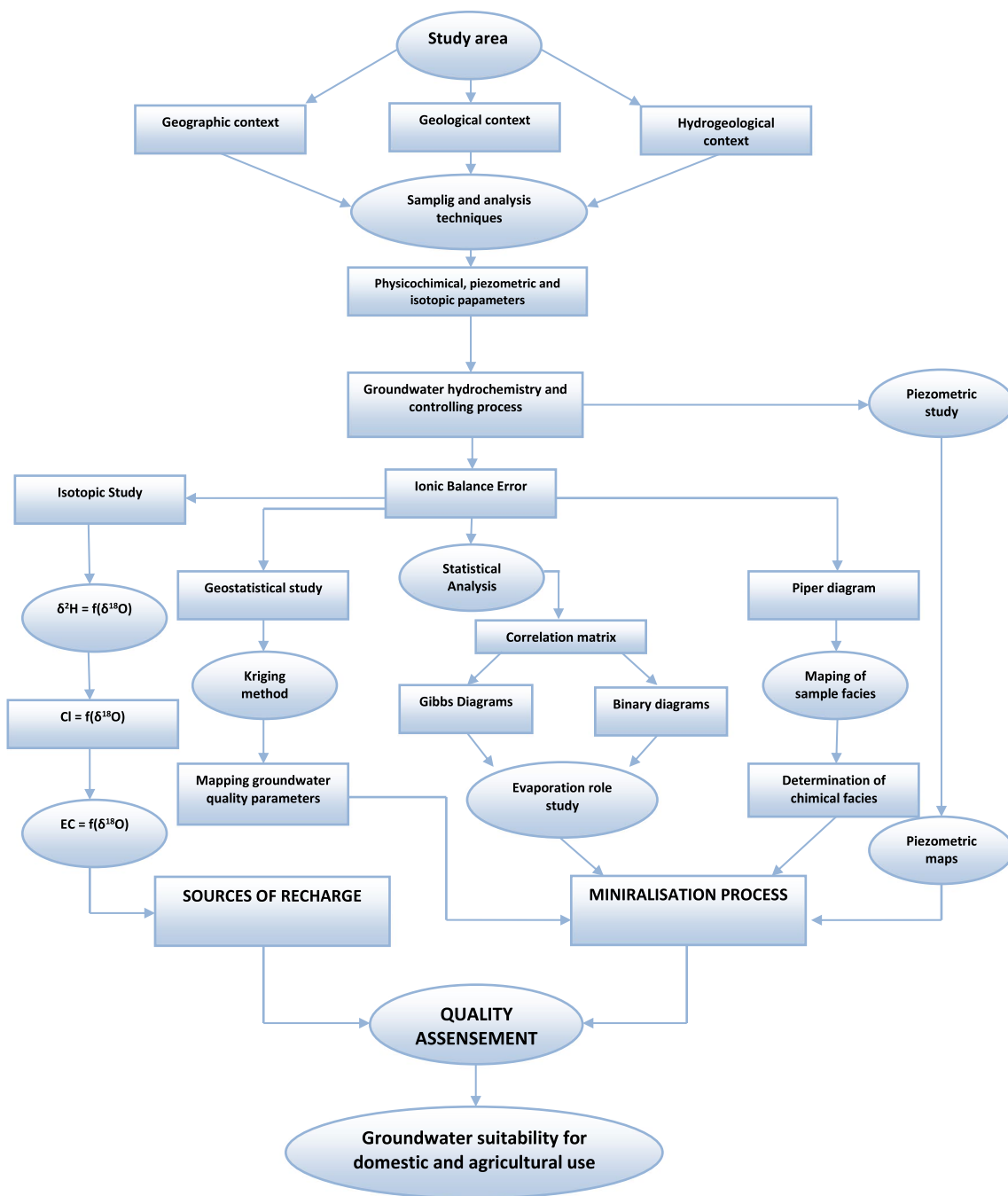


Fig. 3 Methodological steps of the research process

is controlled by solid phase balance. PHREEQC V.2 (Parkhurst and Appelo 1999) was used to calculate the following water minerals saturation indices: calcite (CaCO<sub>3</sub>), dolomite (CaMg (CO<sub>3</sub>)<sub>2</sub>), anhydrite (CaSO<sub>4</sub>), gypsum (CaSO<sub>4</sub>·2H<sub>2</sub>O), and halite (NaCl). Mineral saturation index is obtained from Eq. (1) (Appelo and Postma 2005; Yidana et al. 2007).

$$IS = \log\left(\frac{PAI}{KT}\right) \tag{1}$$

where PAI is a product of ion activity of the chemical element in solution and KT is the equilibrium constant of the considered reaction to T temperature (K). This index is interpreted as follows:

- $IS < 0$  means the water is undersaturated with respect to the mineral in question.
- $IS = 0$  means the water is in equilibrium with the mineral.
- $IS > 0$  means a solution oversaturated with respect to the mineral in question.

Ion exchange processes can be evaluated using the chloro-alkaline index (Schoeller 1977). This index is the ratio between exchanged ions and ions of the same nature originally existing in water. It is given by the following expression:

$$CAI = r \frac{Cl^- - (K^+ + Na^+)}{Cl^-} \quad (2)$$

All values are expressed in milliequivalent per liter. This index defines ionic exchanges between groundwater and surrounding host-rocks:

- $CAI = 0$ , no exchange;
- $CAI < 0$ ,  $Ca^{2+}$  and  $Mg^{2+}$  of groundwater are exchanged by  $Na^+$  and  $K^+$  of hosting rocks;
- $CAI > 0$ ,  $Na^+$  and  $K^+$  of groundwater are exchanged by  $Ca^{2+}$  and  $Mg^{2+}$  of hosting rocks.

### Evaluation of groundwater quality for irrigation purposes

Groundwater containing salts can be unsuitable for irrigation. This risk is determined using absorbable sodium value (sodium absorption ratio (SAR)). For the same conductivity, the magnitude of the risk is proportional to the value of the coefficient. SAR is defined by the following relationship where all ions are expressed in milliequivalent per liter.

$$SAR = \frac{(Na^+ + K^+)}{\sqrt{\frac{(Ca^{2+} + Mg^{2+})}{2}}} \quad (3)$$

Richards (1954) proposed the groundwater classification according to the EC and SAR values. This diagram is very useful and reliable to characterize the suitability for irrigation. However, it cannot be used to assess a risk of salinization or sodization.

### Electrical conductivity evolution

Electrical conductivity (EC) is an important parameter in groundwater quality characterization, where salinity is dependent on natural and/or anthropogenic factors. Figure 4 shows the EC values distribution map. In April 2005 (Fig. 4 a), the low EC values (0.66 to 0.75 mS/cm) are located in the center of the plain. They are surrounded with the EC

medium values (0.75 to 1.00 mS/cm). The rest of the plain is characterized by a high EC values (1.00 to 2.25 mS/cm). In September 2005 (Fig. 4 b), the area of low EC values is located in the center of the plain, while the area of medium EC values surrounds it and extends to the west. The rest of the plain is characterized by a high EC values. In May 2017 (Fig. 4 c), a medium EC area appeared around the industrial zone in the center over a radius ranging from 1.5 to 2.5 km, while the rest of the plain is characterized by a high EC values. In October 2017 (Fig. 4 d), medium EC area extends throughout the center of the plain. The rest of the plain is characterized by high EC values.

The evolution for the EC values depends on several essential factors, including evaporation linked to the piezometric surface proximity in some places (in the western and north-eastern areas of the plain), the geological factor or proximity of lands endowed with evaporitic rocks, as well as marls in piedmonts of the Blidean Atlas which may explain the increase in electrical conductivities in the regions located just downstream; anthropogenic factor also impact through pollution infiltration in industrial zones in the southwestern and in the northeastern and uncontrolled discharge points. Also, seawater intrusion in the Algiers Bay region is a main cause in the increases in the EC in the coastal part of the study area.

## Results and discussions

### Piezometric study

The piezometric study was based on the monitoring of four surveys of the following wet and dry periods: April 2005, September 2005, May 2017, and October 2017. The first examination of the established piezometric maps (Fig. 5) and (Fig. 6) do not reveal any change in the morphology of the piezometric contour lines during the wet and dry periods, but a significant drop in the piezometric depth was noticed from the year 2005 to the year 2017. In general, piezometric levels are decreasing from the North to the South, which means that groundwater flow takes place in a North–South direction which substantially coincides with the direction of the four wadis (Mazafran, Chifa, El Harrach, and El-Hamiz wadis) that cross the plain. Also, we can see the existence of the drawdown area in the northeastern characterized by the groundwater overexploitation.

In the central part, groundwater contours are distant, showing low hydraulic gradients which are around  $2.7 \times 10^{-3}$  in September 2005 and  $6.6 \times 10^{-3}$  in October 2017. This indicates that the formations are more and more coarse and regular. They are linked to the formation of dominant gravel and pebbles in this region. These values vary just a little

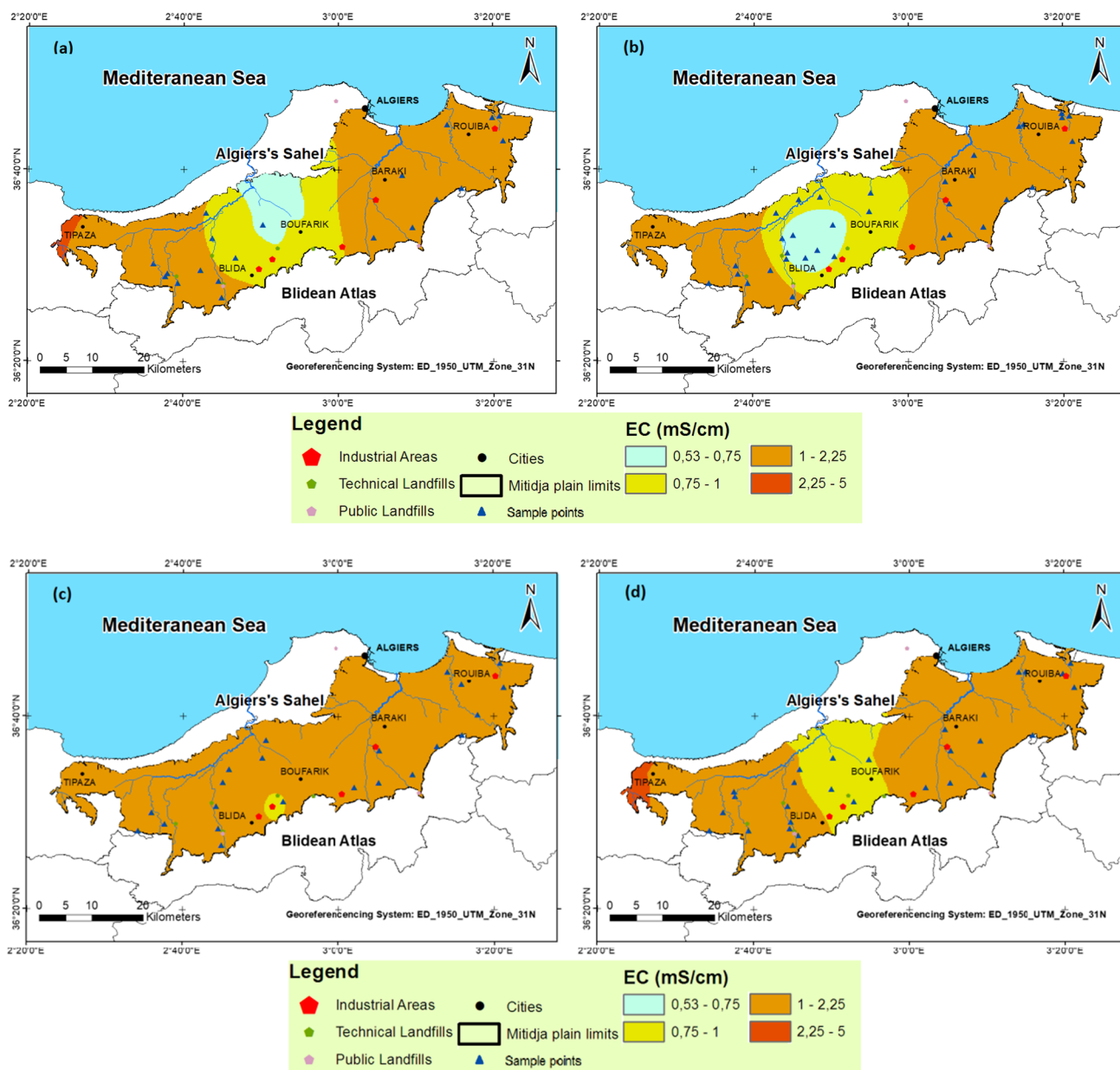


**Fig. 4** Electric conductivity distribution maps (mS/cm) in the study area: **a** April 2005 and **b** September 2005; **c** May 2017 and **d** October 2017

across different sectors. This region indicates a better permeability of the aquifer.

In the upstream part of the study area (the Blidean Atlas piedmont), the piezometric curves are closer showing a high hydraulic gradient ranging from  $1.1 \times 10^{-2}$  in April 2005 to  $2 \times 10^{-2}$  in October 2017.

The piezometric surface depth is variable along the plain. The lowest values are recorded in the eastern region, which vary from 11 m in April 2005 to 18 m in October 2017. Moreover, the highest values are recorded in the Blidean Atlas piedmonts and west zone, which vary from 76 m (April 2005) to 67 m (October 2017), respectively.

Finally, these maps indicate, probably, the appearance of the seawater intrusion phenomenon in the northeastern part of the study area (the Algiers bay) which is caused by the overexploitation of the aquifer in this zone and particularly in El Hamiz wellfield.

**Ionic balance error**

The ionic balance of all samples collected wet and dry period of years 2005 and 2017 has been checked. Correlation between anion and cation concentrations in all samples is high ( $R^2 \geq 0.98$ ). Similarly, the correlation between total



**Fig. 5** Piezometric maps of the study area: **a** April 2005 and **b** September 2005

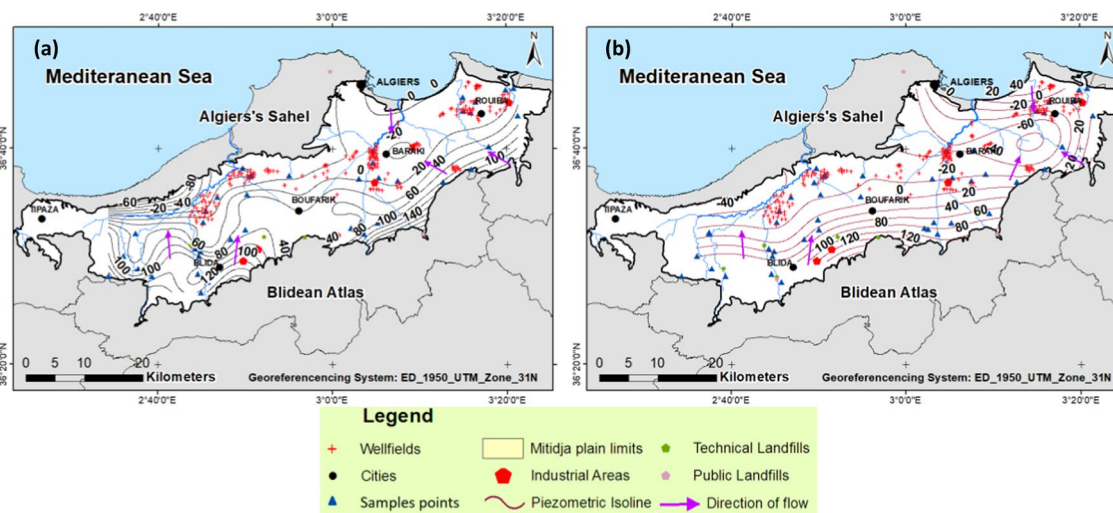
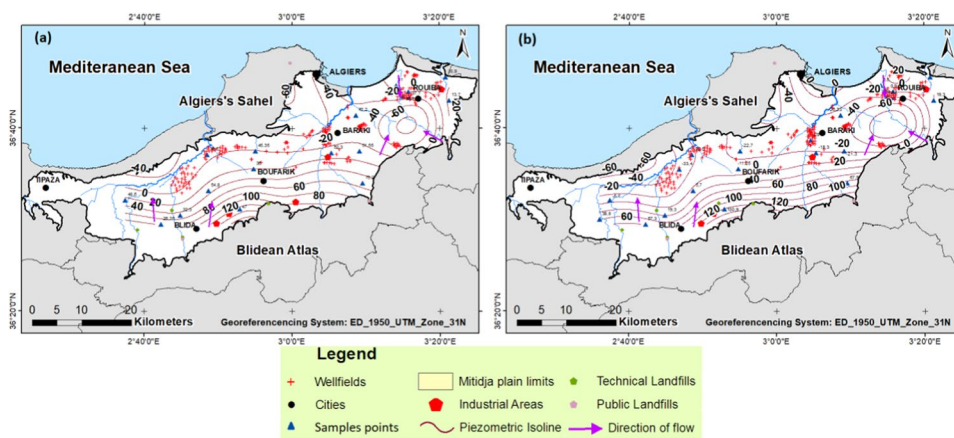


**Fig. 6** Piezometric maps of the study area: **a** May 2017 and **b** October 2017

concentration and dry residue is very high ( $R^2 \geq 0.94$ ). All the hydrochemical analyses were validated according to their charge balance error (CBE):

$$\text{Charge Balance Error (CBE \%)} = \frac{\sum \text{cations} - \sum \text{anions}}{\sum \text{cations} + \sum \text{anions}} \times 100 \tag{4}$$

Out of 104 sample analyses, 102 samples have a  $\text{CBE} \pm 5\%$ . The remaining analyses of CBEs were between 5 and 9%. It can therefore be concluded that analytical procedures are very good.

**Statistical analysis of physicochemical data**

Tables 1 and 2 show the descriptive statistics of the hydrochemical data for the years 2005 and 2017. In most cases, the standard deviation is lower than the average. Standard deviation characterizes the dispersion of the values around average. This indicates that the physicochemical parameters

are not widely dispersed. They thus highlight a certain hydrochemical homogeneity of the groundwater samples in the study area for all the years.

**Correlation matrix**

Pearson’s correlation matrix was used to analyze the relationships between the elements (Tables 3, 4, 5, and 6). During the period 2017/WP, sodium/potassium ( $R=0.70$ ) and chlorides ( $R=0.77$ ). During 2017/DP, the correlation coefficient slightly increases between dry residue and calcium ( $R=0.83$ ), magnesium ( $R=0.78$ ), sodium/potassium ( $R=0.80$ ), chlorides ( $R=0.79$ ), and sulfates ( $R=0.78$ ). The same evolution occurs in both periods WP and DP in 2005.

These relationships identify clearly the main elements that contribute to groundwater mineralization.

The highest correlations between elements combine  $\text{Cl}^-$  and  $\text{Na}^+$  where the  $R=0.87$  in 2005/WP,  $R=0.84$  in 2005/DP,  $R=0.8$  in 2017/WP, and  $R=0.61$  in 2017/

**Table 1** Variation in groundwater physicochemical parameters for the year 2005

Element	Wet period					Ionic balance	Dry period					Ionic balance
	Min	Max	Mean	Standard deviation	CV		Min	Max	Mean	Standard deviation	CV	
Ca <sup>2+</sup> (mg/L)	41.1	233.5	142.9	62.0	0.43	− 1%	41.4	254.4	136.2	56.5	0.41	2%
Mg <sup>2+</sup> (mg/L)	18.8	84.6	45.4	19.3	0.42		13.8	106.4	38.4	23.4	<b>0.61</b>	
Na <sup>+</sup> + K <sup>+</sup> (mg/L)	18.0	207.0	87.3	51.7	0.59		10.0	300.0	77.4	64.9	<b>0.84</b>	
Cl <sup>−</sup> (mg/L)	30.0	530.0	163.0	126.4	0.78		30.0	652.5	152.8	132.6	<b>0.87</b>	
SO <sub>4</sub> <sup>2−</sup> (mg/L)	19.0	562.5	213.1	130.4	<b>0.61</b>		40.0	445.0	164.3	98.2	<b>0.60</b>	
HCO <sub>3</sub> <sup>−</sup> (mg/L)	166.2	435.5	281.2	77.3	0.27		102.8	434.0	258.4	94.5	0.37	
NO <sub>3</sub> <sup>−</sup> (mg/L)	0.0	229.2	73.5	64.1	0.87		4.0	145.0	43.7	32.0	<b>0.73</b>	
EC (mmhos/cm)	0.5	2.8	1.4	0.6	0.44		0.4	2.6	1.2	0.6	0.48	
pH	6.8	7.9	7.3	0.3	0.04		7.0	8.5	7.5	0.4	0.05	

**Table 2** Variation in groundwater physicochemical parameters for the year 2017

Element	Wet period					Ionic balance (%)	Dry period					Ionic balance (%)
	Min	Max	Mean	Standard deviation	CV		Min	Max	Mean	Standard deviation	CV	
Ca <sup>2+</sup> (mg/L)	18.6	280.4	142.5	56.1	0.39	3%	24.2	250.5	136.3	58.7	0.43	2%
Mg <sup>2+</sup> (mg/L)	0.0	63.1	24.2	17.3	<b>0.72</b>		12.1	155.9	45.0	32.4	<b>0.72</b>	
Na <sup>+</sup> + K <sup>+</sup> (mg/L)	22.0	133.0	75.8	37.2	0.49		34.0	185.0	98.5	47.6	0.48	
Cl <sup>−</sup> (mg/L)	37.0	353.0	142.9	83.9	0.59		34.0	737.5	176.6	139.3	<b>0.79</b>	
SO <sub>4</sub> <sup>2−</sup> (mg/L)	0.1	291.0	95.4	92.9	<b>0.97</b>		0.0	432.0	165.7	115.0	<b>0.69</b>	
HCO <sub>3</sub> <sup>−</sup> (mg/L)	91.5	488.0	310.5	101.8	0.33		79.3	552.1	307.7	122.5	0.40	
NO <sub>3</sub> <sup>−</sup> (mg/L)	5.0	91.0	42.1	25.0	0.59		7.0	94.0	41.3	24.2	0.59	
EC (mmhos/cm)	0.4	2.2	1.3	0.5	0.38		0.4	3.0	1.4	0.6	0.45	
pH	7.6	8.3	8.0	0.2	0.03		7.0	8.5	7.7	0.3	0.04	

**Table 3** Correlation matrix between variables in 2005/DP

Variables	Ca <sup>2+</sup>	Mg <sup>2+</sup>	Na <sup>+</sup> + K <sup>+</sup>	Cl <sup>−</sup>	SO <sub>4</sub> <sup>−2</sup>	HCO <sub>3</sub> <sup>−</sup>	NO <sub>3</sub> <sup>−</sup>	EC	pH
Ca <sup>2+</sup>	<b>1</b>								
Mg <sup>2+</sup>	0.40	<b>1</b>							
Na <sup>+</sup> + K <sup>+</sup>	0.42	0.41	<b>1</b>						
Cl <sup>−</sup>	0.48	<b>0.68</b>	<b>0.84</b>	<b>1</b>					
SO <sub>4</sub> <sup>−2</sup>	<b>0.65</b>	<b>0.75</b>	0.47	0.49	<b>1</b>				
HCO <sub>3</sub> <sup>−</sup>	<b>0.73</b>	− 0.06	0.18	− 0.02	0.29	<b>1</b>			
NO <sub>3</sub> <sup>−</sup>	0.53	0.20	0.41	0.53	0.05	0.25	<b>1</b>		
EC	<b>0.77</b>	<b>0.74</b>	<b>0.82</b>	<b>0.89</b>	<b>0.77</b>	0.34	0.50	<b>1</b>	
pH	− 0.04	0.40	0.38	0.33	0.32	− 0.16	− 0.14	0.30	<b>1</b>

DP, respectively. Other significant correlations are found between Cl<sup>−</sup> and Mg<sup>2+</sup> (*R* = 0.68 in 2005/WP and *R* = 0.82 in 2017/DP), SO<sub>4</sub><sup>2−</sup> and Mg<sup>2+</sup> (*R* = 0.84 in 2005/WP, *R* = 0.75 in 2005/DP), and Cl<sup>−</sup> and Ca<sup>2+</sup> (*R* = 0.7 in 2005/WP and *R* = 0.68 in 2017/DP).

However, the relationship Na<sup>+</sup> vs. Cl<sup>−</sup> suggests the halite dissolution in groundwater, which causes the release of equal concentrations of sodium and chloride in the solution:



High relations between Cl<sup>−</sup> vs. Mg<sup>2+</sup> and Cl<sup>−</sup> vs. Ca<sup>2+</sup> suggest that the cations exchange may also influence considerably subsurface water composition. The positive and significant correlations between sulfate and calcium, sodium, and magnesium with *R* values ranging from 0.63 to 0.75 for the 2005/WP, 2005/DP, 2017/WP, and 2017/DP periods

**Table 4** Correlation matrix between variables in 2005/WP

Variables	Ca <sup>2+</sup>	Mg <sup>2+</sup>	Na <sup>+</sup> +K <sup>+</sup>	Cl <sup>-</sup>	SO <sub>4</sub> <sup>-2</sup>	HCO <sub>3</sub> <sup>-</sup>	NO <sub>3</sub> <sup>-</sup>	EC	pH
Ca <sup>2+</sup>	<b>1</b>								
Mg <sup>2+</sup>	0.54	<b>1</b>							
Na <sup>+</sup> +K <sup>+</sup>	<b>0.61</b>	0.50	<b>1</b>						
Cl <sup>-</sup>	<b>0.70</b>	0.46	<b>0.87</b>	<b>1</b>					
SO <sub>4</sub> <sup>-2</sup>	<b>0.68</b>	<b>0.84</b>	0.44	0.37	<b>1</b>				
HCO <sub>3</sub> <sup>-</sup>	0.31	0.03	0.26	0.13	-0.12	<b>1</b>			
NO <sub>3</sub> <sup>-</sup>	0.55	0.17	0.42	0.28	0.32	0.19	<b>1</b>		
ECE	<b>0.88</b>	<b>0.70</b>	<b>0.87</b>	<b>0.88</b>	<b>0.70</b>	0.24	0.51	<b>1</b>	
pH	-0.31	0.05	-0.31	-0.36	-0.08	0.08	-0.42	-0.31	<b>1</b>

**Table 5** Correlation matrix between variables in 2017/DP

Variables	Ca <sup>2+</sup>	Mg <sup>2+</sup>	Na <sup>+</sup> +K <sup>+</sup>	Cl <sup>-</sup>	SO <sub>4</sub> <sup>-2</sup>	HCO <sub>3</sub> <sup>-</sup>	NO <sub>3</sub> <sup>-</sup>	EC	pH
Ca <sup>2+</sup>	<b>1</b>								
Mg <sup>2+</sup>	0.53	<b>1</b>							
Na <sup>+</sup> +K <sup>+</sup>	0.60	0.45	<b>1</b>						
Cl <sup>-</sup>	<b>0.60</b>	<b>0.82</b>	<b>0.61</b>	<b>1</b>					
SO <sub>4</sub> <sup>-2</sup>	<b>0.79</b>	0.56	<b>0.63</b>	0.42	<b>1</b>				
HCO <sub>3</sub> <sup>-</sup>	0.55	0.08	0.40	-0.03	0.42	<b>1</b>			
NO <sub>3</sub> <sup>-</sup>	0.26	0.47	0.56	0.42	0.39	0.19	<b>1</b>		
EC	<b>0.86</b>	<b>0.81</b>	<b>0.79</b>	<b>0.85</b>	<b>0.78</b>	0.38	0.53	<b>1</b>	
pH	-0.43	-0.31	-0.31	-0.22	-0.30	-0.51	-0.25	-0.40	<b>1</b>

**Table 6** Correlation matrix between variables in 2017/WP

Variables	Ca <sup>2+</sup>	Mg <sup>2+</sup>	Na <sup>+</sup> +K <sup>+</sup>	Cl <sup>-</sup>	SO <sub>4</sub> <sup>-2</sup>	HCO <sub>3</sub> <sup>-</sup>	NO <sub>3</sub> <sup>-</sup>	EC	pH
Ca <sup>2+</sup>	<b>1</b>								
Mg <sup>2+</sup>	0.19	<b>1</b>							
Na <sup>+</sup> +K <sup>+</sup>	0.21	0.45	<b>1</b>						
Cl <sup>-</sup>	0.38	0.29	<b>0.80</b>	<b>1</b>					
SO <sub>4</sub> <sup>-2</sup>	<b>0.67</b>	0.42	0.48	0.27	<b>1</b>				
HCO <sub>3</sub> <sup>-</sup>	<b>0.68</b>	0.35	0.06	0.20	0.28	<b>1</b>			
NO <sub>3</sub> <sup>-</sup>	0.36	0.22	-0.10	-0.08	0.29	0.09	<b>1</b>		
EC	<b>0.76</b>	0.56	<b>0.72</b>	<b>0.77</b>	<b>0.66</b>	0.59	0.15	<b>1</b>	
pH	-0.12	0.21	-0.03	-0.05	-0.06	-0.12	0.12	-0.09	<b>1</b>

suggests that these elements can have a common origin and can originate from the dissolution of evaporitic salt formations. The gypsum (CaSO<sub>4</sub>·2H<sub>2</sub>O) is an evaporite element present in the study area. Gypsum dissolution reaction releases sulfate and calcium ions:



Other less significant correlations between dry residue vs. bicarbonates and dry residue vs. nitrates suggest that the groundwater high salinity is due to the saline formations such as gypsum. However, human activity related to agriculture can also contribute to these elements. In the studied plain, farmers widely use potassium, sulfate, ammonium,

and phosphate-based fertilizers (Imerzoukène and Walraevens 1999; DSA-Blida 2003; Boudi 2005; Hadjoudj et al. 2014). In addition, the nitrates are to a lesser degree correlated with all chemical elements.

### Binary diagrams

The Na<sup>+</sup>/Cl<sup>-</sup> ratio has often been used to identify the mechanism of salinity acquisition. Na<sup>+</sup> and Cl<sup>-</sup> ions show a good correlation ( $r=0.87$ ,  $r=0.84$ ) in WP/2005 and DP/2005, respectively, and in WP/2017 and DP/2017 ( $r=0.8$ ,  $r=0.61$ , respectively), indicating that Na<sup>+</sup> and largely Cl<sup>-</sup> are derived from the dissolution of diffused halite in fine-textured sediments. However, a notable characteristic of the Mitidja

aquifer is the enrichment in  $\text{Cl}^-$  compared to  $\text{Na}^+$ . This excess can be explained by the existence of the dissolution of halite. And this ion can also have an anthropogenic origin such as pollution or even the intrusion of seawater towards the aquifer. Indeed, urban wastewater is discharged untreated into the environment and can reach groundwater by infiltration (Chabaca et al. 2007; Hadjoudj et al 2014). The increase in  $\text{Cl}^-$  contents that accompanied the low  $\text{Na}^+$  contents is due to the phenomenon of base exchange, because the bed-rock clays can release  $\text{Ca}^{2+}$  ions after having fixed the  $\text{Na}^+$ .

The  $\text{HCO}_3^-$  ion is weakly correlated with  $\text{Mg}^{2+}$  ( $r=0.03$ ,  $r=-0.006$ ) in WP/2005 and DP/2005, respectively, and in WP/2017 and DP/2017 ( $r=0.35$ ,  $r=0.08$ , respectively) and  $\text{Ca}^{2+}$  ( $r=0.31$  in WP/2005 and  $r=0.55$  in DP/2017), indicating that the dissolution of carbonate rocks (calcite, dolomite) is not the only source for these elements.

The correlation of  $\text{SO}_4^{2-}$  with these two elements is significant with  $\text{Ca}^{2+}$  ( $r=0.68$ ,  $r=0.65$ ) in WP/2005 and DP/2005, respectively, and in WP/2017 and DP/2017 ( $r=0.67$ ,  $r=0.79$ , respectively) and with  $\text{Mg}^{2+}$  ( $r=0.84$  in WP/2005 and  $r=0.75$  in DP/2005). This shows that these elements ( $\text{Ca}^{2+}$ ,  $\text{Mg}^{2+}$ , and  $\text{SO}_4^{2-}$ ) are partly derived by the dissolution of gypsum.

The ratios of  $\text{Ca}^{2+}$  vs  $\text{SO}_4^{2-}$ ,  $\text{Ca}^{2+}$  vs  $\text{HCO}_3^-$ , and  $\text{Ca}^{2+}$  vs  $\text{Mg}^{2+}$  show a large excess of  $\text{Ca}^{2+}$  (Figs. 7 and 8); this indicates that the origin of  $\text{Ca}^{2+}$  is not only the dissolution of calcite and gypsum and confirms thus the hypothesis of a contribution of  $\text{Ca}^{2+}$  by ion exchange following the basic reaction, such as the following:  $\text{Ca}^{2+} - \text{Clay} + 2\text{Na}^+$  (water)  $\rightarrow \text{Ca}^{2+}$  (water) +  $2\text{Na}^+ - \text{Clay}$ .

## Evaporation role

Evaporation effect on the mineralization processes of the Mitidja groundwater is studied using the relation between the ratio ( $\text{Na}^+/\text{Cl}^-$ ) and dry residue in 2017. During both periods (Fig. 9), the ratio  $\text{Na}^+/\text{Cl}^-$  remains more or less constant highlighting a significant effect of evaporation on groundwater mineralization. A slight decrease of the  $\text{Na}^+/\text{Cl}^-$  ratio can be noticed caused probably by ions exchanges processes investigated below.

The Gibbs diagrams (Gibbs 1970) of the two periods of 2005 and 2017 show that the majority of samples are located in the upper part of the graphs with the presence of two groups (Fig. 10) for the all observed periods: (i) the first group shows a mineralization influenced, especially, by the action of the sea and by a low level for evaporation and (ii) the second group shows a mineralization influenced by the processes of water–rock interaction and by the phenomena of evaporation. From these results, it can be concluded that the groundwater of the Mitidja plain may be the consequence

of evaporation; influence of the sea and water–rock interaction of the geological formations make up this plain.

## Nitrate concentration evolution

Figures 11 and 12 show the nitrate concentration distributions in the study area. In April 2005 (Fig. 11 a), 2/3 of the study area has a nitrate concentrations above the WHO standard ( $\leq 50$  mg/L) where the concentration values range from 50 to about 200 mg/L. It can be explained by the excessive use of fertilizers and uncontrolled discharges. The high concentrations are recorded in the East of the study area. In September 2005 (Fig. 11 b), the nitrate concentrations decrease considerably in the study area, while the average concentrations are observed in the eastern region. This decrease in concentration compared to the previous period is due to seasonal change in agricultural practices with a reduced use of the nitrate concentrations (Boudi 2005; Imache et al. 2007). In May 2017 (Fig. 12 c and d), there is a drop in nitrate concentrations across the whole plain except in the East and the West. This is due to the new irrigation techniques used and the control of the fertilizers by the agricultural services.

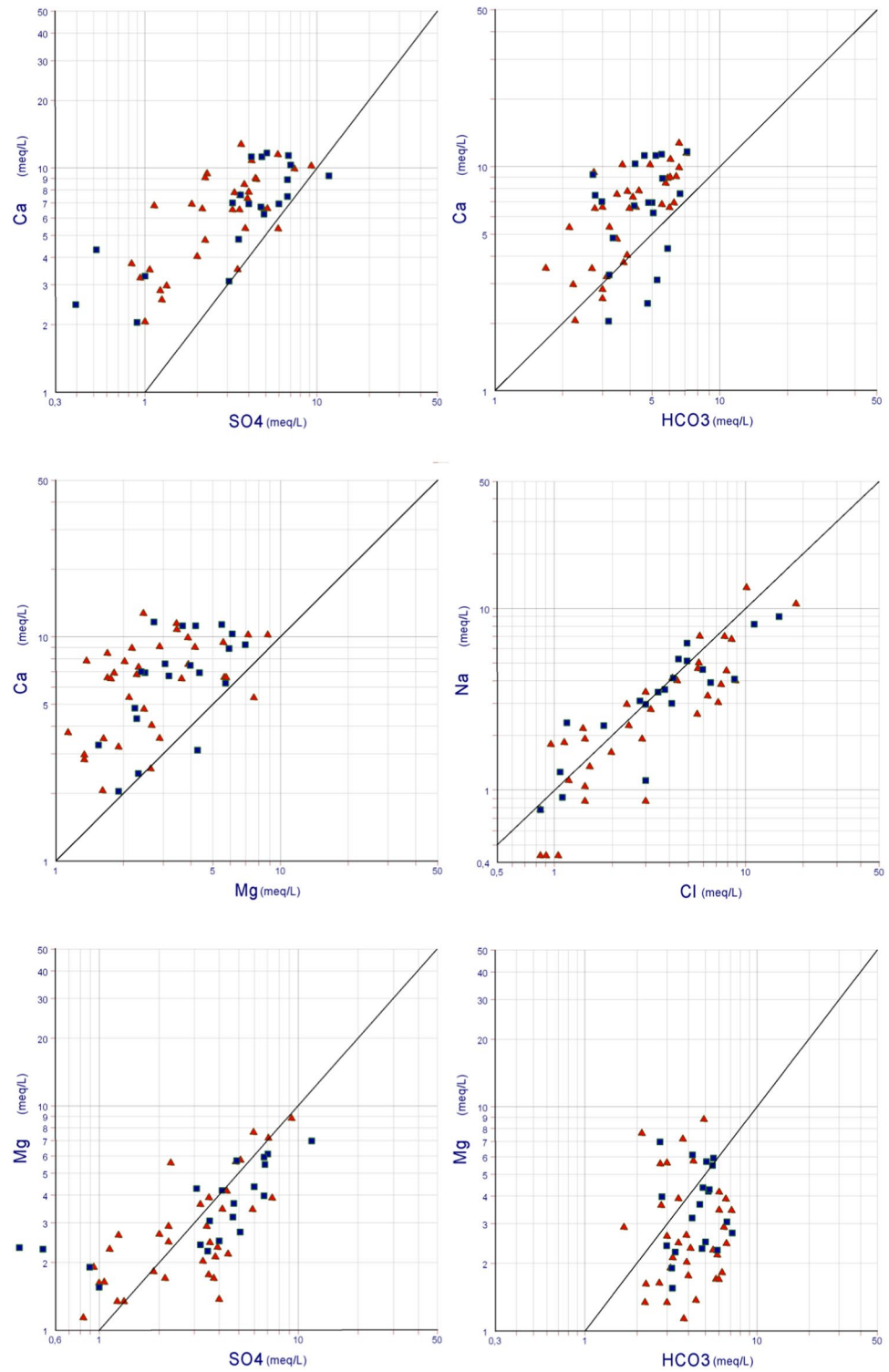
Moreover, the aquifer is very sensitive to the nitrate pollution due mainly to the abusive use of fertilizers, manure, and pesticides in agriculture, especially in the western and northeastern regions where market gardening is practiced contrary to the center zone which is characterized by arboriculture. This pollution is materialized by the uncontrolled discharges from domestic and industrial activity near the urban regions.

## Determination of chemical facies

Interpretation of the hydrochemical data for the 2 years (2005 and 2017) was carried to analyze the chemical facies of the Mitidja alluvial aquifer, their evolution in the time, and the natural conditions of their origin.

The Piper diagrams established for the two periods of wet and dry water periods in 2005 and 2017 (Fig. 13) contribute to represent the many analyzes authorizing grouping of chemical facies. The projection of the chemical analysis results in this diagram clearly shows that the set of point clouds presents a dominance of chloride and bicarbonate ions for the anions, whereas the calcium ion is the cation which marks the majority of the samples and is followed by the sodium cation. This reveals the dominance of the calcium bicarbonate facies followed by the calcium-chloride facies in DP/2005 on the global diagram with an appearance of the sodium-chloride facies, while we find the three facies: bicarbonate calcium, chloride-calcium and sulphate-calcium in WP/2005. In 2017, some development may be noticed, with the emergence of a sodium-chloride pole, linked with

**Fig. 7** Relations between the main major elements in 2005 (red points: dry period, blue points: wet period)

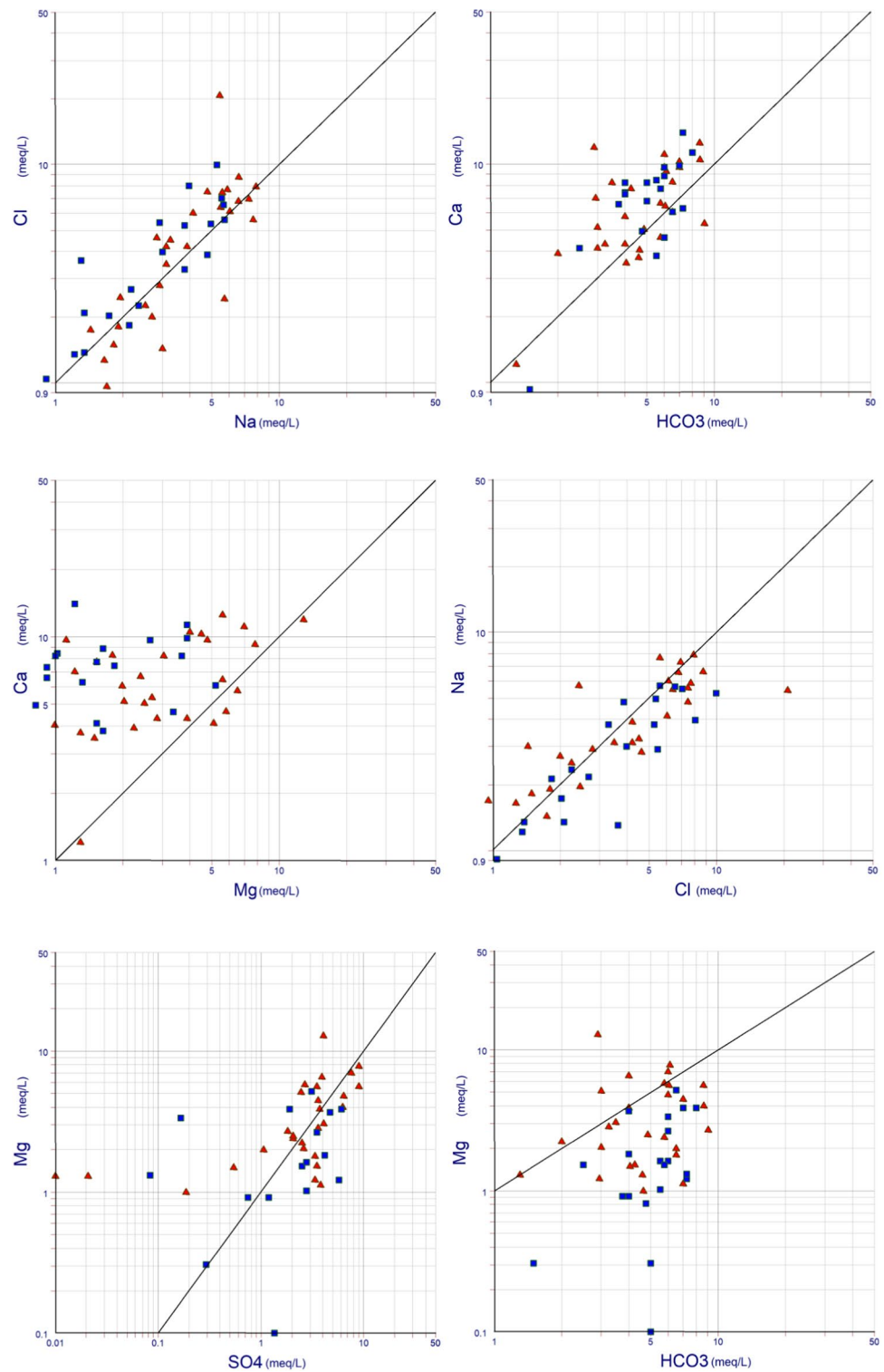


groundwater degradation by seawater intrusion and other sources of contamination (uncontrolled discharges, ...).

Figures 14 and 15 show the spatial distribution of the chemical facies in the groundwater in 2005 and 2017 periods. In April 2005 (Fig. 14 a), three facies are noticed in the plain: (1) sulfate–calcium facies in the Blidean Atlas

piedmont. Its origin is probably geological related to the base exchanges with saliferous formations upstream. Exchanged elements would then migrate towards the plain according to groundwater flow. Also, this facies can have an anthropogenic origin if it is found near the cities or industrial zones; (2) bicarbonate–calcium facies is found in

**Fig. 8** Relations between the main major elements in 2017 (red points: dry period, blue points: wet period)



the center of the plain, due to the carbonate-bearing rock dissolution located in the Blidean Atlas upstream from which groundwater is drained to the center of the plain; (3) chloride-calcium facies is found very rarely. It is located much more near industrial zones of the study area.

In September 2005 (Fig. 14 b), a calcium-bicarbonate facies is more visible in the center of the plain, due to the geological processes and groundwater recharge via the carbonate Blidean Atlas piedmont (limestone and dolomites). A chloride-calcium facies is observed near the industrial

**Fig. 9** Relation between the ratio ( $\text{Na}^+/\text{Cl}^-$ ) and the dry residue for the DP and WP/2017

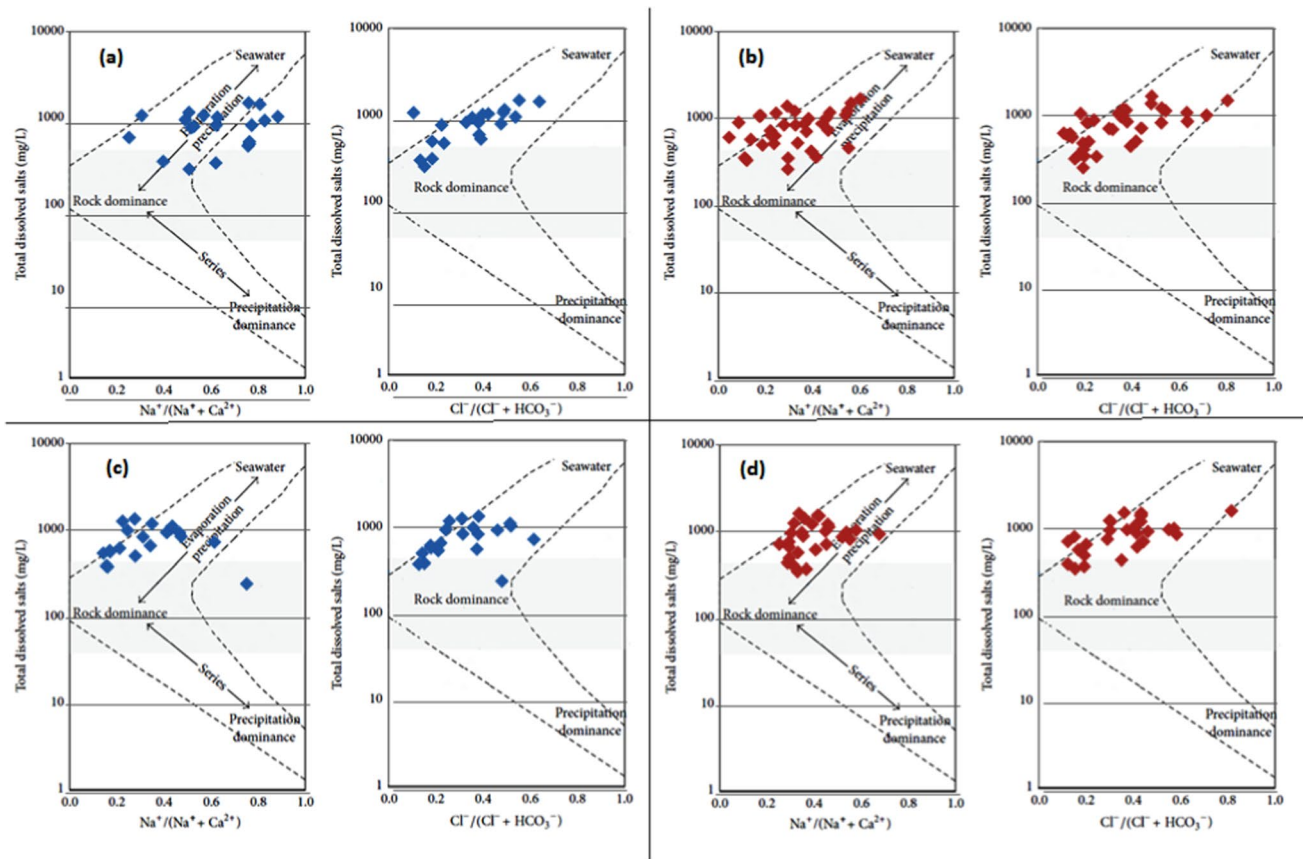
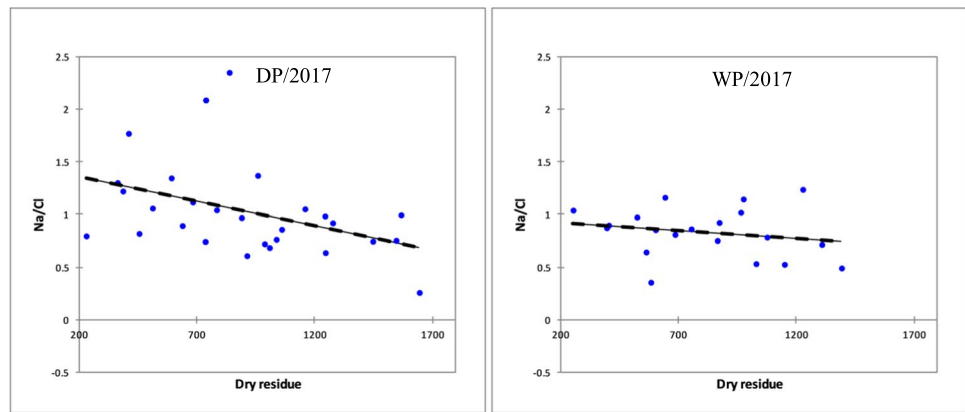


**Fig. 10** Gibbs diagrams: **a** WP/2005, **b** DP/2005, **c** WP/2017, and **d** DP/2017

zones and along the wadis draining the discharges of the large urban groups (Semar, El Harrach, Reghaia, Mazafan, and Bouroumi wadis).

In May and October 2017 (Fig. 15 c and d), a bicarbonate-calcium facies is more abundant in the study area, but the sodium-chloride facies is clearly observed near the industrial zones (anthropogenic origin) and in the Algiers bay (northeastern part), caused by the seawater intrusion.

### Mineralization processes

Dissolved species and their relationships can reveal the origin of solutes and processes that generated the observed composition of the groundwater (Aboubaker et al. 2013; Diaw et al. 2010; Madene et al. 2020; Sujatha and Reddy 2003). These relationships are examined for 2005 and 2017 in wet and dry periods.

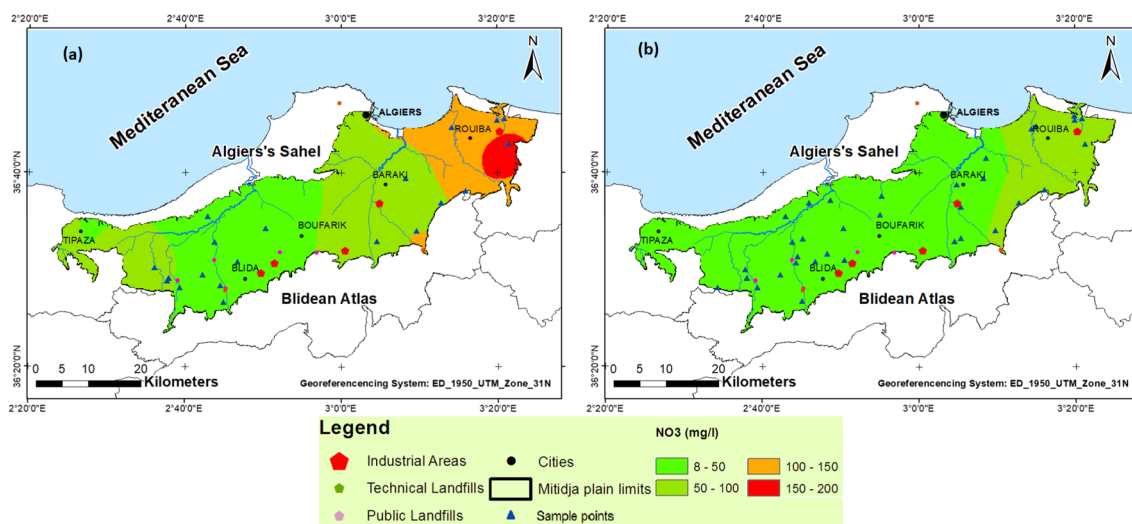


Fig. 11 Nitrate distribution maps in the study area: a April 2005 and b September 2005

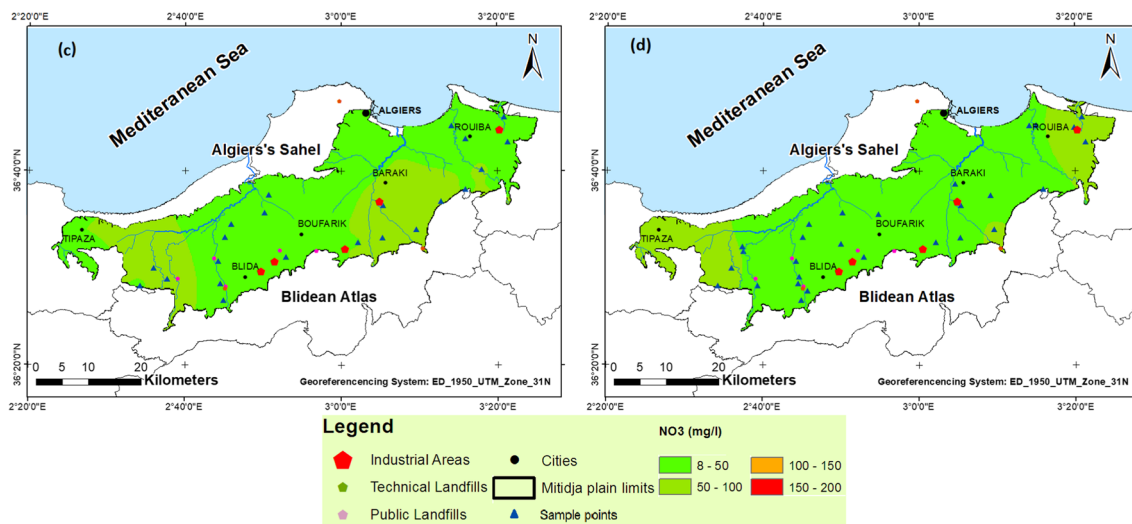
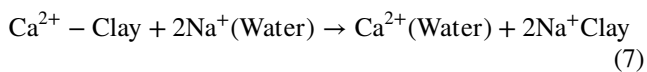


Fig. 12 Nitrate distribution maps in the study area: c May 2017 and d October 2017

The  $\text{Na}^+$  vs.  $\text{Cl}^-$  relationship was often used to identify salinity acquisition mechanism. Significant linear relations are highlighted in 2005 and 2017, indicating that both elements result from the dissolution of halite in the quaternary sediments of the plain. However, at places, high  $\text{Cl}^-$  concentrations are noted compared to  $\text{Na}^+$  (Fig. 16). Excess of  $\text{Cl}^-$  can be related to seawater intrusion (Bachtouli and Comte 2019; Zamiche et al. 2018) and/or infiltration of urban wastewater without prior treatment (Madene et al. 2020). Defect of  $\text{Na}^+$  comes also from the base exchanges processes in which  $\text{Ca}^{2+}$  is released from the substratum clays and exchanged with  $\text{Na}^+$  from the groundwater.

$\text{HCO}_3^-$  does not display any significant relationship with the alkaline earth,  $\text{Ca}^{2+}$  and  $\text{Mg}^{2+}$ , suggesting that the

carbonate-bearing rocks (calcite, dolomite) are not the only source for these elements.  $\text{SO}_4^{2-}$  relationships with the alkaline earth,  $\text{Ca}^{2+}$  and  $\text{Mg}^{2+}$ , are quite significant, which shows that these elements ( $\text{Ca}^{2+}$ ,  $\text{Mg}^{2+}$ ,  $\text{SO}_4^{2-}$ ) come partly from gypsum dissolution which are found in the south (Blidean Atlas piedmont). The  $\text{Ca}^{2+}$  vs  $\text{SO}_4^{2-}$ ,  $\text{Ca}^{2+}$  vs  $\text{HCO}_3^-$ , and  $\text{Ca}^{2+}$  vs  $\text{Mg}^{2+}$  relationships show an important excess of  $\text{Ca}^{2+}$ . This indicates that the  $\text{Ca}^{2+}$  origin is not only calcite and gypsum dissolution but confirms the hypothesis of a contribution of the  $\text{Ca}^{2+}$  by ion exchange following the basic reaction, such as the following:





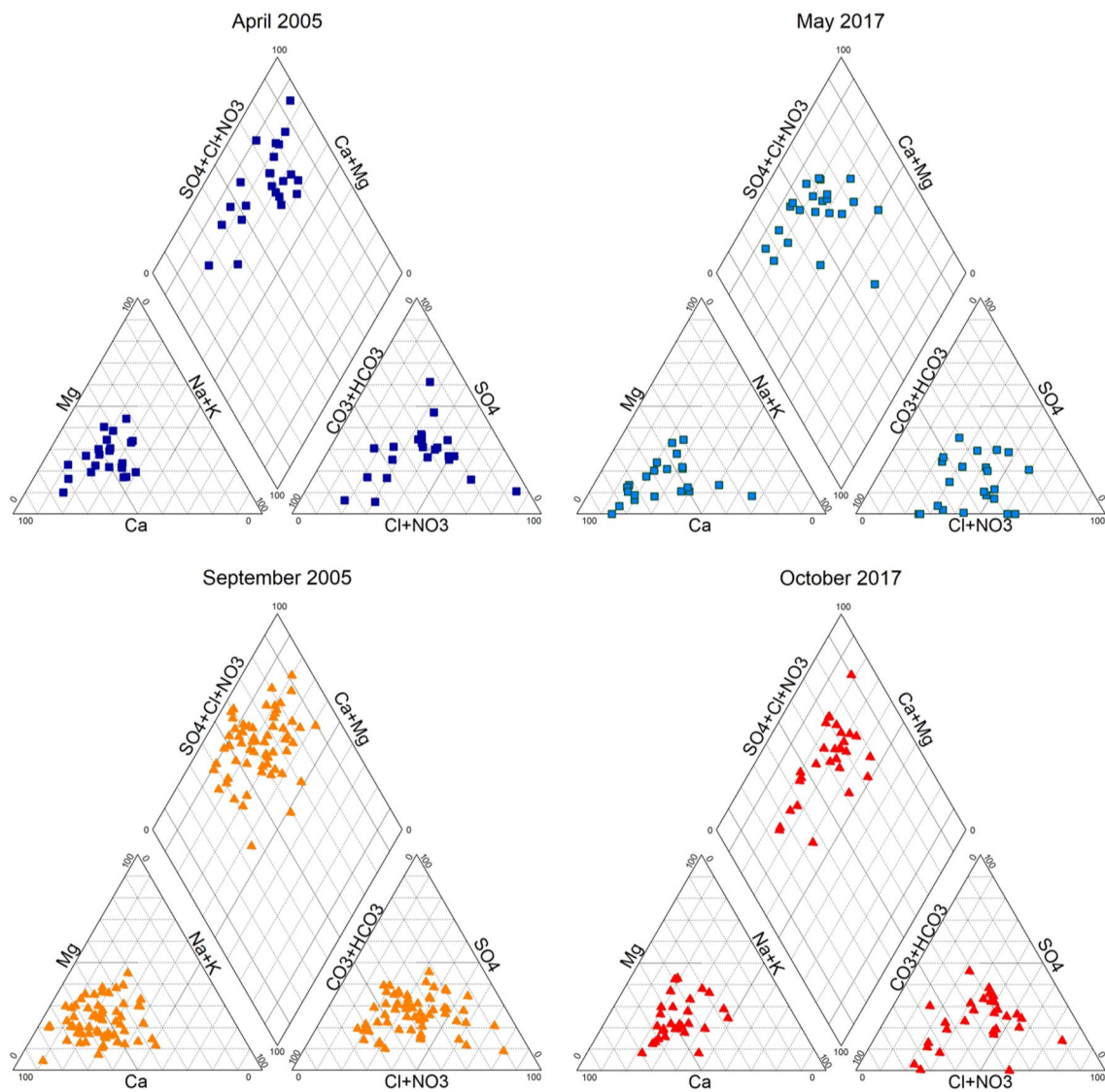


**Fig. 13** Piper plot showing the groundwater chemical types

The  $\text{Na}^+$  ion can exchange the  $\text{Ca}^{2+}$  and  $\text{Mg}^{2+}$  ions adsorbed in exchangeable sites of clay minerals, which leads to the increase in  $\text{Ca}^{2+}$  and  $\text{Mg}^{2+}$  and the decrease in  $\text{Na}^+$  in groundwater.

The knowledge of the variations in groundwater chemistry during its flow through the aquifer is essential. The ion exchanges between groundwater and aquifer rocks were analyzed with the  $\text{Ca}^{2+} + \text{Mg}^{2+}$  vs  $\text{SO}_4^{2-} + \text{HCO}_3^-$  diagram (Fig. 17). In  $\text{Ca}^{2+} + \text{Mg}^{2+}$  vs  $\text{SO}_4^{2-} + \text{HCO}_3^-$  diagram, the points around the equilibrium straight line ( $\text{Ca}^{2+} + \text{Mg}^{2+} = \text{SO}_4^{2-} + \text{HCO}_3^-$ ) suggest that these ions are results of the calcite, dolomite, and gypsum dissolutions (Cerling et al. 1989; Datta and Tyagi 1996; Rajmohan and Elango 2004). When the base exchanges is the dominant process, points will move to the left due to an important excess of  $\text{Ca}^{2+} + \text{Mg}^{2+}$  compared

to  $\text{SO}_4^{2-} + \text{HCO}_3^-$ . In this study, most points are on the  $\text{Ca}^{2+} + \text{Mg}^{2+}$  side (Fig. 17), suggesting the base exchanges are the major hydrogeochemical process operating in this aquifer. For this, the ion exchange process is further examined using the Chloro-Alkaline Index (CAI) (Schoeller 1977; Rachid 2020).

The CAI, defined by Schoeller (1977), is the ratio between exchanged ions and ions of the same nature originally existing in groundwater. It is given by the following expression:

$$CAI = r \frac{\text{Cl}^- - (\text{K}^+ + \text{Na}^+)}{\text{Cl}^-} \tag{8}$$

All values are expressed in milliequivalent per liter. This index defines ionic exchange direction between groundwater and surrounding host-rocks. It is interpreted as follows:

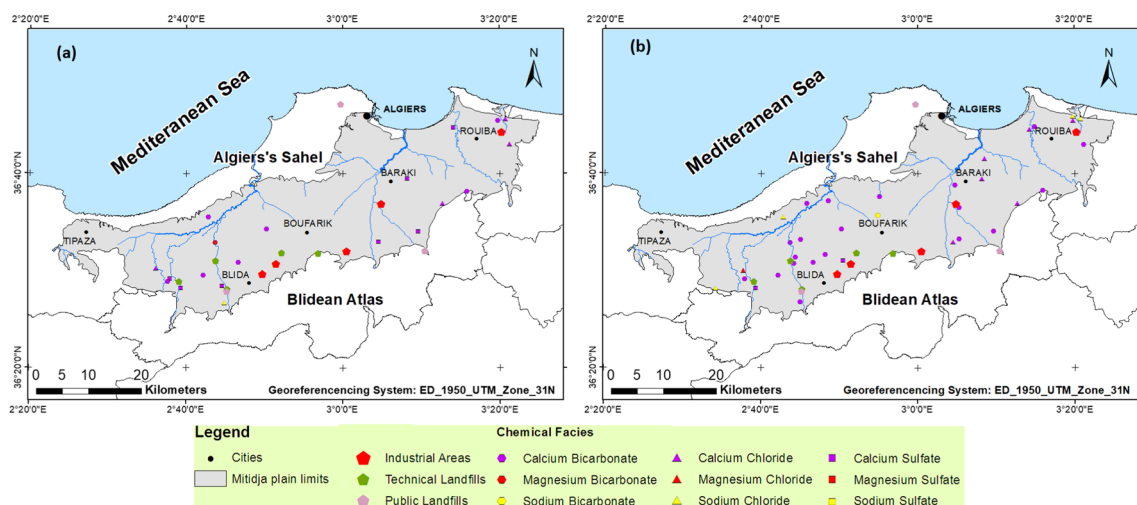


**Fig. 14** Chemical facies distribution maps in the study area: **a** April 2005 and **b** September 2005

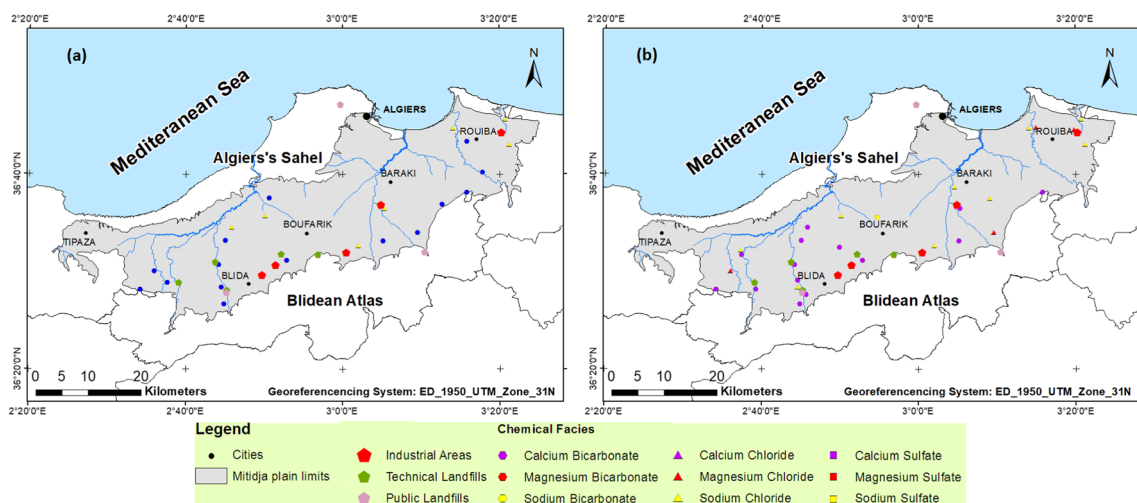


**Fig. 15** Chemical facies distribution maps in the study area: **a** May 2017 and **b** October 2017

- $CAI=0$ , no exchange;
- $CAI<0$ ,  $Ca^{2+}$  and  $Mg^{2+}$  of water are exchanged by  $Na^+$  and  $K^+$  of enveloping formations;
- $CAI>0$ ,  $Na^+$  and  $K^+$  of water are exchanged by  $Ca^{2+}$  and  $Mg^{2+}$  of enveloping formations.

Most samples in the Mitidja alluvial aquifer have a positive index except in the east and in the west. This dominance of positive values reflects the sodium and the potassium replacement in groundwater with calcium and magnesium in surrounding host-rocks.

Mineral saturation indices are very useful in assessing the groundwater quality as water chemistry is controlled by

solid phase equilibria. PHREEQC was used to calculate the following groundwater mineral saturation indices: calcite ( $CaCO_3$ ), dolomite  $CaMg(CO_3)_2$ , anhydrite ( $CaSO_4$ ), gypsum ( $CaSO_4 \cdot 2H_2O$ ), and halite ( $NaCl$ ) during the observation years.

Calculations show that carbonate minerals have different degrees of saturation. Dolomite saturation index ranged from  $-1.76$  to  $-0.76$  in 2005/WP and from  $-0.51$  to  $+3.01$  in 2017/WP, while the calcite intervals vary from  $-0.56$  to  $+1.08$  in 2005/WP and from  $-0.08$  to  $+1.67$  in 2017/WP. Based on the assumption that equilibrium is reached in interval from  $-0.5$  to  $+0.5$ , results show that the calcite has reached equilibrium and the dolomite is in super-saturation condition.

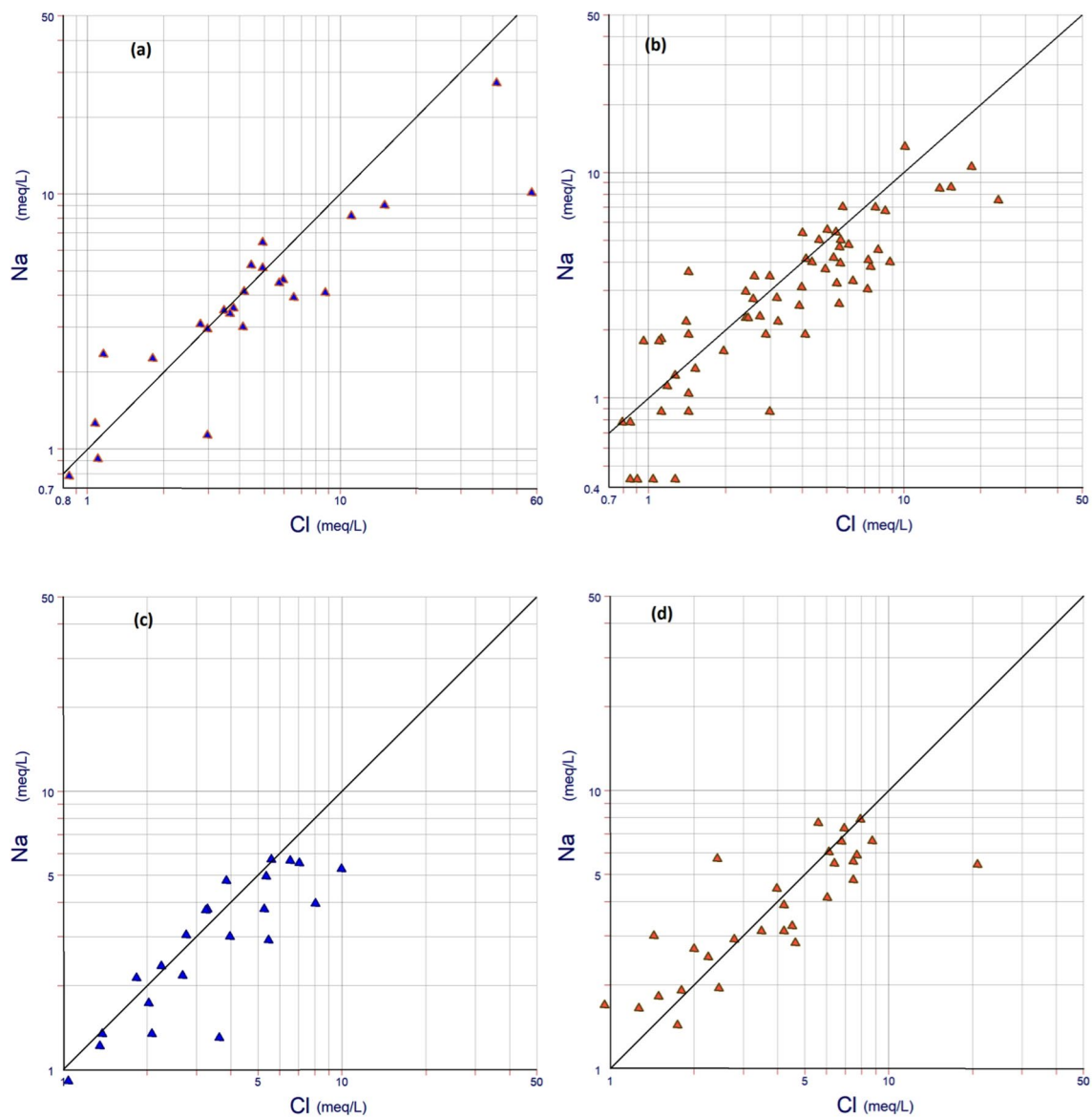


**Fig. 16** Correlation figures between  $\text{Na}^+$  and  $\text{Cl}^-$ : **a** WP/2005, **b** DP/2005, **c** WP/2017, and **d** DP/2017

The evaporitic minerals show degrees of saturation lower than those of the carbonate minerals. The saturation index of gypsum varies from  $-2.39$  to  $-0.76$  in 2005/WP and from  $-5.02$  to  $-0.85$  in 2017/WP, and the saturation index of halite varies from  $-7.84$  to  $-5.6$  in 2005/WP and  $-7.69$  to  $-5.98$  in 2017/WP, which indicates that groundwater is very under-saturated as regards this mineral. For anhydrite, the saturation index ranges from  $-2.63$  to  $-0.98$  in 2005/WP and  $-5.24$  to  $-1.07$  in 2017/WP. In addition, the analysis of the results showed a positive and significant evolution between calcite, dolomite in relation with bicarbonates and gypsum, and the halite with sulfates

and chlorides, respectively, which gives an indication of the different salt dissolutions (Fig. 18).

### Groundwater aptitude for drinking water and irrigation

Groundwater quality is characterized by some physical and chemical parameters, which in turn determine organoleptic property, alone immediately perceptible to the user (Sufet et al. 1995). The parameters taken into account are the total hardness, pH, and mineral substance content generally in dissolved form. Mitidja's alluvial aquifer potability

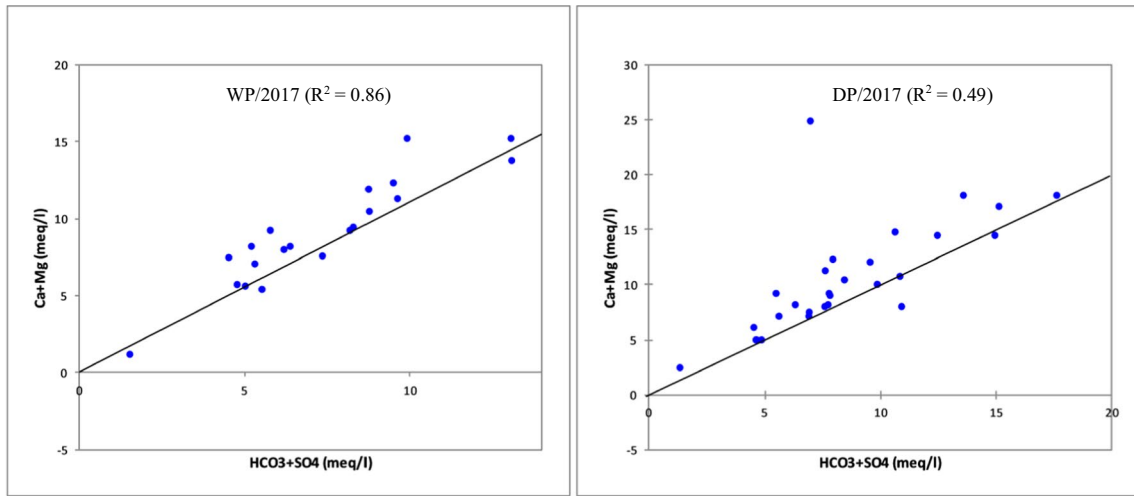


Fig. 17 Relation between ( $Ca^{2+} + Mg^{2+}$ ) and ( $HCO_3^- + SO_4^{2-}$ ) for WP and DP/2017

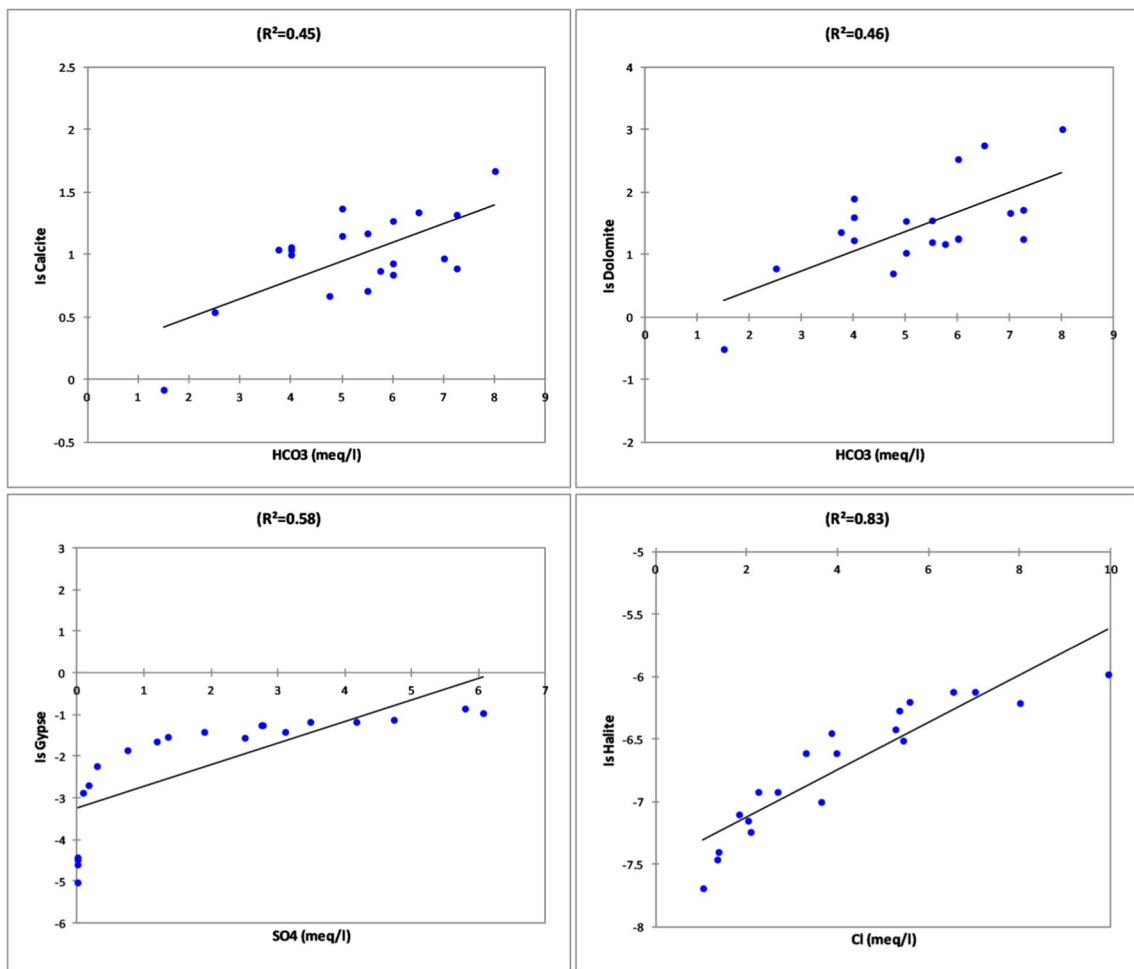


Fig. 18 Variation in saturation index for minerals for WP/2017

**Table 7** Percentage of groundwater samples that have concentrations above WHO standards

Element	WHO standards	Percentage of points with the concentration above WHO standard			
		2005/DP (%)	2005/WP (%)	2017/DP (%)	2017/WP (%)
Ca <sup>2+</sup> (mg/L)	100	76	75	68	73
Mg <sup>2+</sup> (mg/L)	150	0	0	0	0
Na <sup>+</sup> (mg/L)	150	13	17	18	0
K <sup>+</sup> (mg/L)	12	0	−0	0	0
Cl <sup>−</sup> (mg/L)	250	19	21	21	9
SO <sub>4</sub> <sup>2−</sup> (mg/L)	250	13	29	18	9
H CO <sub>3</sub> <sup>−</sup> (mg/L)	250	53	59	61	44
NO <sub>3</sub> <sup>−</sup> (mg/L)	50	44	55	29	27
Dry residue (mg/L)	1500	8	17	11	0
pH	6.5 < pH < 9.2	0	0	0	0

has been assessed according to the international standards (WHO 1993). Contents of the main elements of wet and dry periods in 2005 and 2017 were compared with the WHO (2004) standards and are presented in Table 7.

Table 7 shows that only the potassium contents and pH values are below WHO standards during the 2 years and the dry residue and sodium in 2017/WP. Dry residue contents are at 83% below the WHO standard in 2005/WP. They increase to 91% in 2005/DP and reach 100% in 2017/WP. Sulfates increase from 71% in 2005/WP to 87% in 2005/DP and reach 91% in 2017/WP. Chlorides increase from 79% in 2005/WP to 80% in 2005/DP and reach 90% in 2017/WP. Sodium increase from 83% in 2005/WP to 87% in 2005/DP. In addition, elements that most exceed WHO standards are bicarbonates and nitrates. Also, a clear improvement of water quality in the Mitidja alluvial aquifer is noticed in 2017.

For the agricultural sector, almost 70% of the surface and subsurface water resources are allocated in Mitidja region (Hadjoudj et al. 2014) which contains more than 65% of cultivated cropland over a total area of nearly 1500 km<sup>2</sup>. Agriculture development in this area is currently encountering, apart from scarcity of water resources, new problems such as soil salinization risk which can be assessed by electrical conductivity and that of soil alkalization; it is due to ionic

exchanges (sodium, calcium and magnesium) between water and irrigated soil.

As Mitidja region is agricultural and soil salinization risks can be envisaged, a study of groundwater suitability for irrigation proves necessary, because this region is characterized by an average rainfall (660 mm), a high evaporation (501 mm), and a highly bicarbonate and nitrate concentrations (Table 7).

In this approach, we estimated some salinity parameters in relation to agricultural use for 2005 and 2017. Richards diagram gives the following classes highlighted in Table 8:

- Classes C2S1 and C2S2 characterized by 15% of wells in 2005/WP and 20.58% in 2005/DP, which reached 20% in 2017/WP and 14.29% in 2017/DP, represent a good quality water, usable for the irrigation of all salt-tolerant crops, on well drained or with good permeability soils. They are located in the center of the plain.
- Classes C3S1 and C3S2 characterized by 75% of wells in 2005/WP and 74% in 2005/DP, which reached 80% in 2017/WP and 79% in 2017/DP. They represent a mediocre water, usable only for irrigation of salts tolerant crops, on well drained or with good permeability soils, with a salinity that must be controlled. Class C3S1 characterizes wells located in the center and west of the plain.

**Table 8** Mitidja alluvial aquifer wells distribution (in % of the wells number) according to Richards diagram during the periods 2005/WP, 2005/DP, 2017/WP, and 2017/DP

Class	Water quality	2005/WS		2005/DS		2017/WS		2017/DS	
C2S1	Good	15%	<b>15%</b>	21%	<b>21%</b>	20%	<b>20%</b>	14%	<b>14%</b>
C2S2		0%		0%		0%		0%	
C3S1	Mediocre	75%	<b>75%</b>	74%	<b>74%</b>	80%	<b>80%</b>	79%	<b>79%</b>
C3S2		0%		0%		0%		0%	
C4S1	Poor	10%	<b>10%</b>	0%	<b>6%</b>	0%	<b>0%</b>	7%	<b>7%</b>
C4S2		0%		6%		0%		0%	
C4S3		0%		0%		0%		0%	

- Classes C4S1, C4S2, and C4S3 characterized by 10% of wells in 2005/WP and 6% in 2005/DP, which reached 0% in 2017/WP and 7% in 2017/DP. They indicate a poor-quality water, highly mineralized, which may only be suitable for species that are well tolerant to salts and on well drained and bleached soils. Finally, the majority of wells belonging to the C4S1 and C4S2 classes are located in the east, on the side of Algiers bay; this may be due to the seawater intrusion.

## Isotope results and interpretations

**Oxygen-18 and deuterium** Stable isotopes of water, deuterium ( $^2\text{H}$ ) and oxygen-18 ( $^{18}\text{O}$ ), constitute a powerful tool for determining origin and history of water, recharge areas, and relations between surface water and groundwater. Variations in  $^{18}\text{O}$  and  $^2\text{H}$  water contents are linked to phenomena of condensation, evaporation, steam mixtures (marine-continental-lacustrine), and water/soil exchange reactions (George Darling et al. 2006). Results for isotopic analyzes of oxygen-18 and deuterium in the Mitidja alluvial aquifer are grouped together in Fig. 19. Stable isotopes for 28 groundwater samples taken during the wet and dry periods for the year 2017 were analyzed in order to better understand the groundwater's hydrodynamics in the studied. In the Mitidja alluvial aquifer, groundwater oxygen-18 contents vary between  $-7.27$  and  $-5.22\text{‰}$  vs SMOW (Vienna Standard Mean Ocean Water) with a mean of  $-6.41\text{‰}$  vs SMOW. Deuterium contents range from  $-42.20$  to  $-29.40\text{‰}$  vs SMOW with a mean of  $-35.56\text{‰}$  vs SMOW. The mean isotopic composition of samples ( $-6.41\text{‰}$  for  $\delta^{18}\text{O}$  and  $-35.56\text{‰}$  for  $\delta^2\text{H}$ ) is close to the mean value for precipitation recorded in Algiers during the time-period 2016–2018 ( $-6.3\text{‰}$  for  $\delta^{18}\text{O}$  and  $-36.1\text{‰}$  for  $\delta^2\text{H}$ ) (Khouas et al.

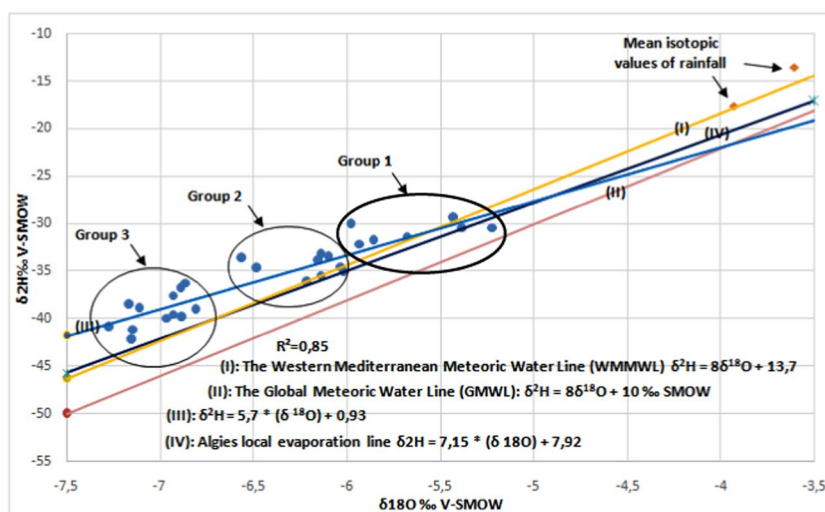
2019). The most enriched values are recorded in the wells located in the northeast part of the plain (on the side of Rouiba-Reghaia industrial zone) and in the southwest part (between El-Afroun, Ahmar El-Ain, and Oued Djer localities), where the evaporation effect was detected. The results have been reported on  $\delta^2\text{H} = f(\delta^{18}\text{O})$  diagram (Fig. 19).

Moreover, the Mitidja groundwater samples are on the whole distributed along the Western Mediterranean Meteoric Water Line (WMMWL) determined by Celle-Jeanton et al. (2001), where the deuterium excess is 14 per mile (WMMWL:  $\delta^2\text{H} = 8 \delta^{18}\text{O} + 14$ ). This implies that the predominant recharge source of the groundwater is the meteoric water originated from west Mediterranean vapor masses. However, the line of best fit between  $\delta^2\text{H}$  and  $\delta^{18}\text{O}$  values is shown by the following equation:  $\delta^2\text{H} = 5.7 \times (\delta^{18}\text{O}) + 0.93$ . The slope of this line is less than 8 (slope value for WMMWL) indicating that the groundwater is likely to have been derived from meteoric water with significant evaporation that has been taken place during or after rainfall (Abu Jabal et al. 2018). In addition, sample fitting line is located above to the left of WMMWL, suggesting that dilution and mixing processes occur in the groundwater (Mokadem et al. 2016); samples showing depleted values in heavy isotopes and deuterium excess greater than 14 are probably impacted by altitude and/or temperature effect (Khouas et al. 2019).

**Relationship between  $\text{Cl}^-$  and  $\delta^{18}\text{O}$**  The correlation between chloride contents and  $\delta^{18}\text{O}$  values is studied to check if the isotopic content enrichment of the water samples is linked to an evaporation process (Bouchaou et al. 1995).

The representation of  $^{18}\text{O}$  contents according to chloride concentrations (Fig. 20) shows that the Mitidja alluvial aquifer can be subdivided into three distinct water groups: (1) the first group present well-homogenized water samples with a content that varies between 34 and 164 mg/L of chlorides where the values of  $\delta^{18}\text{O}$  are comprised between  $-7.27$

**Fig. 19** Oxygen 18-deuterium relationship in the Mitidja alluvial aquifer for DP/2017



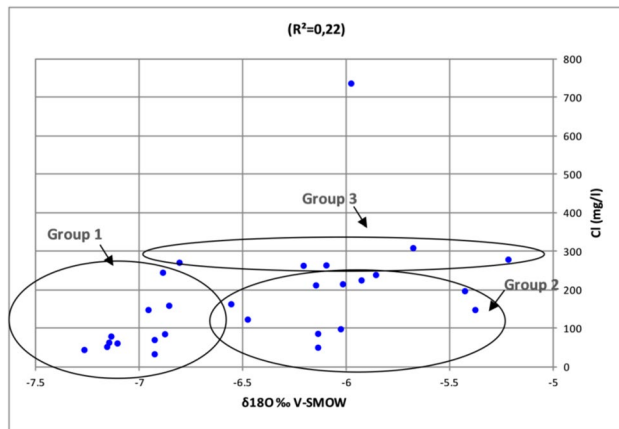


**Fig. 20** Relationship between chloride contents and  $\delta^{18}\text{O}$  for the DP/2017

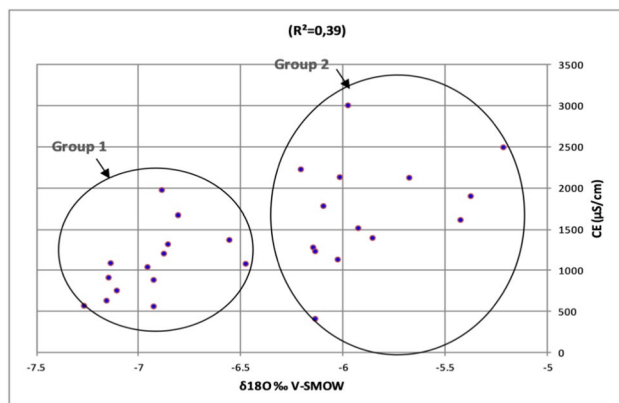


**Fig. 21** Relationship between EC and  $\delta^{18}\text{O}$  for the DP/2017

and  $-6.86\text{‰}$ ; (2) the second group presents the evaporated water samples which are characterized by the oxygen-18 enrichment with a content that varies between 51 and 240 mg/L of chlorides, and the values of  $\delta^{18}\text{O}$  comprised between  $-6.88\text{‰}$  and  $-5.43\text{‰}$ ; and (3) the last category of evaporated water corresponds to the samples located in the central part of the plain and in the Blidean Atlas piedmonts which proves that evaporation exists. This third group contains a chloride contents between 246 and 310 mg/L with the values of  $\delta^{18}\text{O}$  ranging from  $-6.89$  to  $-5.22\text{‰}$ . This category corresponds to the groundwater located in the west and northeast regions. However, the weak correlation between the chloride contents and the values of  $\delta^{18}\text{O}$  ( $R^2=0.22$ ) shows that the solution concentration by evaporation is not the only cause of the increase in the groundwater salinity. The three groups show a rate of 35.71%, 32.14%, and 14.26% of the samples analyzed, respectively.

**Relationship between EC and  $\delta^{18}\text{O}$**  Effect of water evaporation is also highlighted by the electrical conductivity diagram depending on  $\delta^{18}\text{O}$  of groundwater.

Graphic of EC variation depending on  $\delta^{18}\text{O}$  concentrations (Fig. 21) shows that a relationship  $\delta^{18}\text{O}$ -EC suggests a different origin of salinization. We notice that water points located in the west and northeast regions and in the downstream zone of Blidean Atlas piedmonts have significantly higher EC values. These water points indicate salinization which could be the result of dissolution by deep water of evaporite and marl formations which are confirmed by the hydrogeochemical study. Furthermore, in this graph, the Mitidja alluvial groundwater is divided into two individualized group: (a) In the first group, water points have average EC and stable isotopes depleted (from  $-7.27$  to  $-6.81\text{‰}$  vs SMOW for oxygen-18). This group represents 50% of the samples analyzed, and (2) the second group is made up of water characterized by medium to moderate EC, but a little more enriched contents in stable isotopes (from  $-6.48$  to  $-5.22\text{‰}$  vs SMW for oxygen-18). The water of this group which is distinguished by salinization could be the result of evaporitic deposits dissolution, anthropogenic activity characterized by uncontrolled urban and industrial discharges, seawater intrusion, and evaporation phenomena. This group represents 43% of the samples analyzed. Finally, the relationship between  $\delta^{18}\text{O}$ -EC suggests a different origin of salinization and, consequently, confirms the salinity acquisition by the double standard of evaporation and dissolution of evaporitic formations by groundwater.

## Conclusion

The main mineralization processes are as follows: (1) dissolution of evaporite rocks as well as marls in the Blidean Atlas piedmont, (2) to be verified seawater intrusion in the northeastern region (the Algiers bay) of the plain, and (3) the infiltration of irrigation water loaded with salts and fertilizers into the irrigated areas of the plain and the processes of base exchanges.

The results show that the groundwater is characterized by a high salinity and two dominant facies according to the Piper method: The first is bicarbonate-calcium facies observed in the center of the study area. The second is chloride-calcium facies which is found near to the industrial zones. This facies is of anthropogenic origin. We also note the occurrence of the chloride-sodium facies in the northeastern part of the study area (the Algiers bay) at a distance ranging from 1.5 to 3.5 km from the coast which is due to the seawater intrusion confirmed on the electrical conductivity maps and on the piezometric maps which indicate a reverse

groundwater flow from the coast towards the aquifer in the Hamiz wellfield (excessive pumping rates).

Moreover, the high salinity of the groundwater in other areas of the plain is mainly due to chlorides, leaching of chlorinated fertilizers and salts not used by plants. Nitrate pollution of the groundwater exceeds the threshold of 50 mg/L recommended by WHO.

The isotopic analysis of oxygen-18/deuterium relations showed the existence of three types of freshwater: (1) water that is the result of the direct infiltration (recharge) of rainfall, (2) the return of irrigation water, and (3) the water dissolution of evaporitic rocks located in the Blidean Atlas piedmont. The content of  $^{18}\text{O}$  versus  $\text{Cl}^-$  of this aquifer would reflect a mixture of recharge water from current precipitation over the basin and saline water from interaction with evaporite rocks and seawater intrusion in the northeast region. The  $\delta^{18}\text{O}$ -EC relationship suggests a different origin of salinization, which confirms that the salinity is due to both evaporation and dissolution by groundwater of carbonates and evaporite formations; hence, both processes occur in the Mitidja alluvial aquifer. Groundwater mineralization and salinization are due to the dissolution process of carbonates and evaporitic formations, especially during the dry periods.

Understanding of the Mitidja alluvial aquifer origin and its mineralization processes represents a major step forward for future management decisions with a view to preserving this essential water resource for the social and economic development of this region and the application of this approach in the similar worldwide regions.

**Author contribution** All authors contributed to the study conception and design. Material preparation, data collection, and analysis were performed by Samir Yahiaoui. The first draft of the manuscript was written by Samir Yahiaoui and Mohamed Meddi. Mohamed Meddi, Moumtaz Razack, Abdelmadjid Boufekane, and Belkacem Samir Bekkoussa commented on previous versions of the manuscript. All authors read and approved the final manuscript.

**Funding** This work was carried out as part of the project ERANET-MED\_WATER-13–166, Groundwater Resilience to Climate Change and High Pressure within an IWRM Approach, funded by the DGRSDT/MESRS, Algeria.

**Data availability** The datasets used and analyzed during the current study are available from the corresponding author on reasonable request.

## Declarations

**Ethical approval** Not applicable.

**Consent to participate** Not applicable.

**Consent for publication** All authors have approved the manuscript and agree with submission to Environmental Science and Pollution Research.

**Competing interests** Authors Samir Yahiaoui, Mohamed Meddi, and Abdelmadjid Boufekane have received research funding from DGRSDT/MESRS (Algeria). Authors Moumtaz Razack and Belkacem Samir Bekkoussa declare they have no financial interests.

## References

- Aboubaker M, Jalludin M, Razack M (2013) Hydrochemistry of a complex volcano-sedimentary aquifer using major ions and environmental isotopes data : Dalha basalts aquifer, southwest of Republic of Djibouti. *Environ Earth Sci* 70(7):3335–3349. <https://doi.org/10.1007/s12665-013-2398-8>
- Abu Jabal MS, Abustan I, Rozaimy MR, El Najar H (2018) The deuterium and oxygen-18 isotopic composition of the groundwater in Khan Younis City, southern Gaza Strip (Palestine). *Environ Earth Sci* 77(4):155. <https://doi.org/10.1007/s12665-018-7335-4>
- Adams SM, Greeley MS (2000) Ecotoxicological indicators of water quality: using multi-response indicators to Assess the health of aquatic ecosystems. *Water Air Soil Pollut* 123:103–115. <https://doi.org/10.1023/A:1005217622959>
- Adimalla N, Li P, Qian H (2018) Evaluation of groundwater contamination for fluoride and nitrate in semi-arid region of Nirmal Province, South India: a special emphasis on human health risk assessment (HHRA) 25(5):1107–1124. <https://doi.org/10.1080/10807039.2018.1460579>
- Ait Ouali A (2007) Synthèse hydrogéologique et vulnérabilité à la pollution du système aquifère quaternaire de la Mitidja (Magister/FSTGAT-USTHB). [https://scholar.google.com/citations?view\\_op=view\\_citation&hl=fr&user=oLFgLssAAAAJ&citation\\_for\\_view=oLFgLssAAAAJ:u-x608ySG0sC](https://scholar.google.com/citations?view_op=view_citation&hl=fr&user=oLFgLssAAAAJ&citation_for_view=oLFgLssAAAAJ:u-x608ySG0sC)
- American Public Health Association (2005) American Water Works Association and Water Pollution Control Federation, Standard methods for the examination of water and wastewater, 4110-B. Ion chromatography with chemical suppression of eluent conductivity, 21st Edition, 2005
- Appelo CAJ, Postma D (2005) *Geochemistry, groundwater and pollution* (2e éd.). CRC Press. <https://doi.org/10.1201/9781439833544>
- Bachtouli S, Comte JC (2019) Regional-scale analysis of the effect of managed aquifer recharge on saltwater intrusion in irrigated coastal aquifers: Long-term groundwater observations and model simulations in NE Tunisia. *J Coast Res* 35(1):91–109. <https://doi.org/10.2112/JCOASTRES-D-17-00174.1>
- Barcelona MJ, Gibb JP, Helfrich JA, Garske EE (1985) Practical guide for ground-water sampling. EPA/600/2–85/104
- Bellon H, Lepvrier C, Raymond D (1977) L'activité éruptive dans l'algérois : Nouvelles données géochronologiques- Persée. [https://www.persee.fr/doc/geolm\\_0397-2844\\_1977\\_num\\_4\\_4\\_1010](https://www.persee.fr/doc/geolm_0397-2844_1977_num_4_4_1010)
- Bouaissa M, Gharibi E, Ghalit M, Taupin JD, El Khattabi J (2021) Identifying the origin of groundwater salinization in the Bokoya massif (central Rif, northern Morocco) using hydrogeochemical and isotopic tools. *Groundw Sustain Dev* 14:100646
- Bouaissa M, Gharibi E, Ghalit M, Taupin JD, Boukich O, El Khattabi J (2022) Groundwater quality evaluation using the pollution index and potential non-carcinogenic risk related to nitrate contamination in the karst aquifers of Bokoya massif, northern Morocco. *Int J Environ Anal Chem* 1–21
- Bouchaou L, Chauve P, Mania J, Mudry J, Michelot J (1995) Apports des traçages artificiel et naturel à la connaissance des circulations et des zones de recharge en région semi-aride : Cas de l'Atlas de Beni Mellal (Maroc). *Revue Des Sciences De L'eau / J Water Sci* 8(1):43–55. <https://doi.org/10.7202/705212ar>
- Bouderbala A, Hadj Mohamed N (2020) Water resources in coastal aquifers of Algeria face climate variability: case of alluvial aquifer



- of Mitidja in Algeria. In: Negm AM, Bouderbala A, Chenchouni H, Barceló D (eds) Water resources in Algeria - part I. The handbook of environmental chemistry, vol 97. Springer, Cham. [https://doi.org/10.1007/698\\_2020\\_529](https://doi.org/10.1007/698_2020_529)
- Boudi M (2005) Vulgarisation agricole et pratiques des agrumiculteurs de la Mitidja [Thesis, INA]. [http://dspace.ensa.dz:8080/jspui/bitstream/123456789/74/1/boudi\\_m.pdf](http://dspace.ensa.dz:8080/jspui/bitstream/123456789/74/1/boudi_m.pdf)
- Boufekane A, Yahiaoui S, Meddi H, Meddi M, Busico G (2021) Modified DRASTIC index model for groundwater vulnerability mapping using geostatistic methods and GIS in the Mitidja plain area (Algeria). *Environ Forensics* 23(5–6):539–556. <https://doi.org/10.1080/15275922.2021.1913674>
- Bouteldjaoui F, Bessenasse M, Taupin JD, Kettab A (2020) Mineralization mechanisms of groundwater in a semiarid area in Algeria: statistical and hydrogeochemical approaches. *J Water Supply Res Technol AQUA* 69(2):173–183. <https://doi.org/10.2166/aqua.2019.116>
- Celle-Jeanton H, Travi Y, Blavoux B (2001) Isotopic typology of the precipitation in the Western Mediterranean Region at three different time scales. *Geophys Res Lett* 28(7):215–218. <https://doi.org/10.1029/2000GL012407>
- Cerling TE, Pederson BL, Von Damm KL (1989) Sodium-calcium ion exchange in the weathering of shales: implications for global weathering budgets. *Geology, GeoScienceWorld*. <https://pubs.geoscienceworld.org/gsa/geology/article-abstract/17/6/552/204924/Sodium-calcium-ion-exchange-in-the-weathering-of>
- Chabaca MN, Isberie C, Messahel M (2007) The policy of water management for irrigation versus the climatic risk to the social and economic constraints: case of Algeria. *La Houille Blanche* 93(4):161–136. <https://doi.org/10.1051/lhb:2007055>
- Datta PS, Tyagi SK (1996) Major ion chemistry of groundwater in Delhi area: chemical weathering processes and groundwater flow regime. *Journal of Geological Society of India (Online Archive from Vol 1 to Vol 78)*, 47(2), Art. 2. <http://isolar.info/index.php/JGSI/article/view/7/177>
- Diaw M, Faye S, Stichler W, Maloszewski P (2010) Isotopic and geochemical characteristics of groundwater in the Senegal River delta aquifer: implication of recharge and flow regime. *Environ Earth Sci* 66:1011–1020. <https://doi.org/10.1007/s12665-010-0710-4>
- DSA-Blida (2003) Statistiques de la Wilaya de Blida, Algérie
- George Darling W, Bath AH, Gibson JJ, Rozanski K (2006) Isotopes in water. In: Leng MJ (ed) *Isotopes in palaeoenvironmental research developments in paleoenvironmental research*, vol 10. Springer, Dordrecht. [https://doi.org/10.1007/1-4020-2504-1\\_01](https://doi.org/10.1007/1-4020-2504-1_01)
- Gibbs RJ (1970) Mécanismes contrôlant la chimie mondiale de l'eau. *Sciences* 170:1088–1090. <https://doi.org/10.1126/science.170.3962.1088>
- Glangeaud L, Aymé A (1935) Carte géologique de l'Algérie à 1/50 000-Arba. <https://medihal.archives-ouvertes.fr/medihal-00787724>
- Hadjoudj O, Bensemmane R, Saoud Z, Reggabi M (2014) Pollution des eaux souterraines de la Mitidja par les nitrates : État des lieux et mesures correctives. *Eur J Water Qual* 45:57–68. <https://doi.org/10.1051/wqual/20140010>
- Imache A, Goulven PL, Bouarfa S, Chabaca M (2007) Evolutions de la demande en eau agricole dans la plaine irriguée de la Mitidja, Algérie. p. 10. <http://hal.cirad.fr/cirad-00259795>
- Imerzoukène S Walraevens K (1999) Simulation of groundwater flow and evolution of the fresh-/salt-water interface in the coastal aquifer of the Mitidja Plain (Algeria). *Natuurwetenschappelijk Tijdschrift*. 79(1–4): 249–262. <https://www.vliz.be/nl/imis?module=ref&refid=27452>
- Khous D, Ait-Amar H, Belaid M, Chorfi H (2019) Geochemical and isotopic assessment of groundwater quality in the alluvial aquifer of the Eastern Mitidja Plain. *Water Resour* 46(3):443–453. <https://doi.org/10.1134/S0097807819030060>
- Madene E, Meddi H, Boufekane A, Meddi M (2020) Contribution of hydrogeochemical and isotopic tools to the management of upper and middle Cheliff aquifers. *J Earth Sci* 31(5):993–1006. <https://doi.org/10.1007/s12583-020-1293-y>
- Meddi M, Hubert P (2003) Impact de la modification du régime pluviométrique sur les ressources en eau du Nord-Ouest de l'Algérie. In: *Hydrology of the Mediterranean and semi arid regions*, IAHS publication, vol 278, pp 229–235
- Mokadem N, Demdoum A, Hamed Y, Bouri S, Hadji R, Boyce A, Laouar R, Sâad A (2016) Hydrogeochemical and stable isotope data of groundwater of a multi-aquifer system: Northern Gafsa basin – Central Tunisia. *J Afr Earth Sc* 114:174–191. <https://doi.org/10.1016/j.jafrearsci.2015.11.010>
- Ouradi L (2014) Contribution à la gestion de l'eau d'irrigation d'un périmètre : Cas du périmètre irrigué Mitidja Est [Thesis]. <http://dspace.ensa.dz:8080/xmlui/handle/123456789/419>
- Parkhurst DL, Appelo CAJ (1999) User's guide to PHREEQC (Version 2): a computer program for speciation, batch-reaction, one-dimensional transport, and inverse geochemical calculations. <https://pubs.er.usgs.gov/publication/wri994259>
- Piper AM (1944) A graphic procedure in the geochemical interpretation of water-analyses. *EOS Trans Am Geophys Union* 25(6):914–928. <https://doi.org/10.1029/TR0251006p00914>
- Rachid G (2020) Adaptation to saltwater intrusion along highly urbanized coastal areas: a DSS-based socioeconomic perspective. <http://scholarworks.aub.edu.lb/handle/10938/21862>
- Rajmohan N, Elango L (2004) Identification and evolution of hydrogeochemical processes in the groundwater environment in an area of the Palar and Cheyyar River Basins, Southern India. *Environ Geol* 46:47–61. <https://link.springer.com/article/10.1007%2Fs00254-004-1012-5>
- Richard LA (1954) Diagnosis and improvement of saline and alkali soil. *Agricultural Handbook* 60. USDA, Washington, DC, p 160
- Rivoirard R (1952) Aperçu sur l'hydrogéologie de la Mitidja. [https://www.editions-gandini.fr/index2.php?page=shop.product\\_details&flypage=flypage.tpl&product\\_id=841&category\\_id=3&option=com\\_virtuemart&Itemid=2](https://www.editions-gandini.fr/index2.php?page=shop.product_details&flypage=flypage.tpl&product_id=841&category_id=3&option=com_virtuemart&Itemid=2)
- Rodier J, Bazin C, Broutin J, Champsaur H, Rodi L (2009) *Water analysis. Natural water. Waste water. Sea water*. 8<sup>ème</sup> Ed. Dunod. Paris : p. 1383
- Scanlon BR, Jolly I, Sophocleous M, Zhang L (2007) Global impacts of conversions from natural to agricultural ecosystems on water resources: quantity versus quality. *Water Resour Res* 43:W03437. <https://doi.org/10.1029/2006WR005486>
- Schoeller H (1977) *Géochimie des eaux souterraines: Vol. Groundwater studies—un guide international pour la recherche et la pratique*. UNESCO
- Semmoud B, Ladhém A (2015) L'agriculture périurbaine face aux vulnérabilités foncières en Algérie. *Territoire en mouvement Revue de géographie et aménagement. Territory in movement Journal of geography and planning* 25–26. <https://doi.org/10.4000/tem.2845>
- Sogreah A (2009) Impact des changements climatiques sur les ressources en eau. Note de synthèse
- Suffet IH, Mallevalle J, Kawczynski E (1995) Advances in taste-and-odor treatment and control. *American Water Works Association*
- Sujatha D, Reddy BR (2003) Quality characterization of groundwater in the south-eastern part of the Ranga Reddy district, Andhra Pradesh, India. *Environ Geol* 44(5):579–586. <https://doi.org/10.1007/s00254-003-0794-1>
- UNESCO (2022) Executive summary. *United Nations World Water Development Report 2022: Groundwater: Making the invisible visible*. <https://www.unesco.org/reports/wwdr/2022/en/download>
- United Nations (2018) *The United Nations world water development report 2018: nature-based solutions for water*. <https://unesdoc.unesco.org/ark:/48223/pf0000261424>

- United Nations (2022) Population | Nations Unies. United Nations; United Nations. <https://www.un.org/fr/global-issues/population>
- WMO (2021) State of the global climate. [https://library.wmo.int/doc\\_num.php?explnum\\_id=11178#:~:text=The%20global%20mean%20temperature%20in,and%20end%20of%20the%20year](https://library.wmo.int/doc_num.php?explnum_id=11178#:~:text=The%20global%20mean%20temperature%20in,and%20end%20of%20the%20year)
- World Health Organization (1993) Guidelines for drinking-water quality (2nd ed)
- World Health Organization (2004) Guidelines for drinking-water, vol. 1, 2004
- Yidana S, Ophori D, Banoeng-Yakubo B (2007) Hydrogeological and hydrochemical characterization of the Voltaian Basin: the Afram Plains area, Ghana. *Environ Geol* 53:1213–1223. <https://doi.org/10.1007/s00254-007-0710-1>
- Zamiche S, Hamaidi-Chergui F, Demiai A, Belaidi M (2018) Identification of factors controlling the quality of groundwater in Mitidja plain (North Algeria) using indexing method and statistical analysis. *J Fundam Appl Sci* 10(1):248. <https://doi.org/10.4314/jfas.v10i1.19>
- Zamiche S (2019) Etude de la qualite physico-chimique et microbiologique en tant qu'indicateurs de la qualite des eaux souterraines dans la plaine de la Mitidja, Thesis, univ-blida1. <http://di.univ-blida.dz:8080/jspui/handle/123456789/8902>
- Zeroual A, Meddi M, Assani AA (2016) Artificial neural network rainfall-discharge model assessment under rating curve uncertainty and monthly discharge volume predictions. *Water Resour Manag* 30:3191–3205. <https://doi.org/10.1007/s11269-016-1340-8>

**Publisher's note** Springer Nature remains neutral with regard to jurisdictional claims in published maps and institutional affiliations.

Springer Nature or its licensor (e.g. a society or other partner) holds exclusive rights to this article under a publishing agreement with the author(s) or other rightsholder(s); author self-archiving of the accepted manuscript version of this article is solely governed by the terms of such publishing agreement and applicable law.

## Authors and Affiliations

Samir Yahiaoui<sup>1</sup> · Mohamed Meddi<sup>1</sup> · Moumtaz Razack<sup>2</sup> · Abdelmadjid Boufekane<sup>1,3</sup>  · Belkacem Samir Bekkoussa<sup>4</sup>

✉ Abdelmadjid Boufekane  
boufekane\_ab@yahoo.fr

<sup>1</sup> National Higher School for Hydraulics, LGEE, Blida B.P.31, 09000 Blida, Algeria

<sup>2</sup> Faculté Des Sciences Fondamentales Et Appliquées, UMR CNRS 7285, Rue Albert Turpain, Bât.B8, 86022 Poitiers Cedex, France

<sup>3</sup> Geo-Environment Laboratory, Department of Geology, Faculty of Earth Sciences and Country Planning, University of Sciences and Technology Houari Boumediene (FSTGAT/USTHB), 16111 Bab Ezzouar, Algiers, Algeria

<sup>4</sup> Laboratoire des Sciences Et Techniques de L'Eau, University Mustapha Stambouli of Mascara, P.O. Box 305, 29000 Mascara, Algeria